

DELFT UNIVERSITY OF TECHNOLOGY

REPORT 17-08

A LITERATURE STUDY ON MODELING INTEGRATED ENERGY SYSTEM
NETWORKS

A.S. MARKENSTEIJN, C. VUIK

ISSN 1389-6520

Reports of the Delft Institute of Applied Mathematics

Delft 2017

Copyright © 2017 by Delft Institute of Applied Mathematics, Delft, The Netherlands.

No part of the Journal may be reproduced, stored in a retrieval system, or transmitted, in any form or by any means, electronic, mechanical, photocopying, recording, or otherwise, without the prior written permission from Delft Institute of Applied Mathematics, Delft University of Technology, The Netherlands.

A Literature Study on Modeling Integrated Energy System Networks

A.S. Markensteijn, C. Vuik

April 24, 2018

Contents

1	Introduction	5
2	Types of network	5
2.1	Gas	6
2.1.1	Physical network	6
2.1.2	Network representation	7
2.1.3	Model	7
2.1.4	Components	11
2.2	Electricity	13
2.2.1	Physical power grid	13
2.2.2	Network representation	14
2.2.3	Model	15
2.2.4	Power loss	21
2.2.5	Distributed slack node approach	21
2.3	Heat	22
2.3.1	District Heating	22
2.3.2	Network representations	24
2.3.3	Model	25
3	Comparison between networks	30
3.1	Models	30
4	Integrated energy networks	33
4.1	Coupling components	33
4.1.1	Models	34
4.2	Coupling between networks	37
4.2.1	Direct coupling	38
4.2.2	Energy hub	40
5	Summary	42

1 Introduction

Traditionally, the energy system consists of separate networks, e.g. a gas network, a power grid, and a heating network, that are designed, operated and controlled separately. In the last years there has been increased interest in the integration of these separate systems into one energy system. The potential advantages of such an integrated system are reduced total carbon emission, increased use of renewable energy, increased flexibility, increased reliability of the electrical power system and reduced capital expenditure [Abeysekera, 2016]. The total carbon emission is reduced due to increased efficiency of the total system, which is mainly due to co-generation of electricity and heat and due to optimizing the operations of the total energy system (as opposed to optimizing the operations of the separate systems). The use of renewable energy is mainly limited by the technical limits of the power grid. When the different networks are integrated into a single system, any excess power generated by a renewable source, that would otherwise be curtailed, can be ‘stored’ in the other networks using converter units such as a power-to-gas unit. Therefore the use of renewables can be increased. The reliability and flexibility can be increased by load shifting. Due to converter units the electricity for a load (i.e. a demand) can for instance be supplied by the gas network, effectively shifting the load from the power grid to the gas network. The capital expenditure can be reduced because an integrated energy systems can provide additional energy supply capacity. This means that the utilization of the existing networks can be increased, and reinforcement work to existing networks can be delayed or reduced.

However, integrated energy systems currently also have disadvantages. First of all, the introduction of converter units and other interdependencies between the different systems leads to more complicated systems that are not well understood and for which no (few) commercial software tools are available [Abeysekera, 2016]. Secondly, the market is currently adjusted to the separate energy networks and not to one integrated system. Finally, the increasing interdependencies can lead to a total system that is more prone to cascade failures.

In order for the integrated energy systems to be designed, operated and controlled effectively, models need to be developed that represent the entire integrated system. The first step of such a model is a model that allows for steady-state flow analysis of an integrated energy system. This literature study will therefore focus on the steady-state flow analysis of the separate and integrated energy systems. In Section 2 the separate networks considered are discussed and the most common models for these individual networks are given. In Section 3 a comparison between the individual networks is given. In Section 4 converter units are introduced and discussed, and the resulting integrated energy systems is discussed, including to models for the integrated system. Finally, some concluding remarks are given in Section 5.

2 Types of network

This section describes the different types of networks that will be considered, namely a gas network, a power grid (electrical network) and a district heating network. For each network, the physical network and the abstraction to a graph are described. Furthermore, one or more of the commonly used models for steady-state flow analysis are given for each network.

The focus of the integrated energy systems will be on regions in the Netherlands. Therefore, all the technical aspects for the separate networks are given with respect to the Dutch networks.

2.1 Gas

2.1.1 Physical network

Wobbes [2015] describes the physical Dutch gas network. A summary of this description is given below. The (Dutch) gas network consist of three main parts; the transmission grid, the regional grid and the distribution grid. It transports two types of gas; low calorific gas (L-gas) which is sometimes also called Groningen gas (G-gas) and high calorific gas (H-gas). The different types of gas will not be taken into account for the steady-state flow analysis. The transmission grid consists of high pressure transmission lines (HTL) and transfers gas throughout the entire country. The HTL consists of a total of approximately 6000 km of pipe lines which have an average diameter of 1 meter, and which operate at pressures between 40 and 67 bar. The HTL is also connected to gas storage sites in the Netherlands and is used for the import and export of gas. The HTL is connected to the regional grid via metering and regulating stations. At these station the pressure is lowered to 7-40 bar. The regional transmission lines (RTL) consists of a total of approximately 6000 km of pipe lines which have an average diameter of 25 cm. The RTL is connected to the distribution network via gas receiving stations. At these stations, the pressure is lowered to approximately 8 bar. The distribution network consists of a total of approximately 127000 km of pipe lines. The distribution grid is itself also divided in a high pressure and a low pressure part. The high pressure distribution grid is connected to the gas receiving stations (i.e. to the RTL) and is used to transport the gas over relatively large distances. The high pressure lines are connected to the low pressure grid via supply stations. At these stations the pressure is lowered to 100 or 30 mbar. The low distribution grid directly delivers the gas to households and small industries. An overview of the

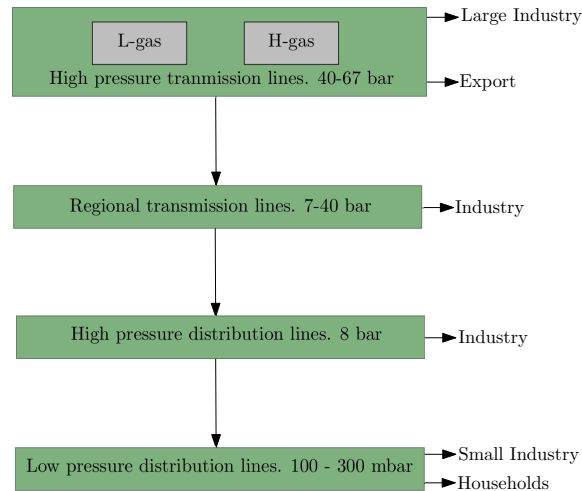


Figure 1: Schematic representation of the gas network in the Netherlands.

gas grid is shown in Figure 1.

Apart from pipe lines, sources (i.e. gas supply) and loads there are three main components in the gas network; compressors, pressure regulators and valves Osiadacz [1987]. Due to friction in the pipe lines the pressure drops during the transportation of gas. To maintain the required pressure compressors are used. At the same time it might be desirable to lower the pressure from a relatively

high pressure to a relatively low pressure, e.g. at a supply station where gas is transferred from the high pressure distribution grid to the low pressure distribution grid. To change the pressure to the required value pressure regulators are used. The third component are the valves. They are used to regulate the gas flow, for instance to prevent flow of gas in a wrong direction, to control the amount of gas flow through a pipe or to cut off certain regions of the network in case of break-down. The components will be discussed in more detail later on.

2.1.2 Network representation

When representing the gas network as a network (i.e. as a graph), nodes and links are introduced. The nodes generally represents a point in the network where gas can enter (sources) or leave (loads) the network or a point in the network where gas is redistributed over multiple lines (junctions). The links are generally used to represent the pipe lines, but they can for instance also be used to represent compressors. A link is also called an edge. A node in a gas network is fully described by two parameters [Osiaacz, 1987]:

- the pressure p
- the (injected) gas flow rate q

Here, the gas flow rate q is the gas volume flow rate. In the rest of this report, both flow rate and flow are used to indicate flow rate. The nodal variable for (injected) gas flow q is the sum of all the flows entering and leaving that node. For the gas network, all nodes are treated the same, except for the slack node, see Table 1. At all the nodes (except the slack node) it is assumed that

Table 1: Node types for gas network

Node type	Number of nodes	Specified parameters	Unknown parameters
slack node	1	p_i	q_i
other node	$N - 1$	q_i	p_i

the injected (or consumed) gas volume flow is given. To ensure that the model will be well defined the pressure is specified at one node instead of the gas flow. This node is called the slack node or reference node. The other function of the slack node is to ensure that the total demand is met, i.e. the amount of gas injected into to slack node is such that the total demand of the gas network can be supplied.

2.1.3 Model

For gas networks, steady-state flow analysis is equivalent to determining the flow through the pipes and the pressure at the nodes for a steady-state situation. For the model commonly used to perform steady-state flow analysis, the following assumptions are made [Osiaacz, 1987]:

- Steady-state flow.
- Isothermal flow.
- Kinetic energy changes in the pipe are neglected.
- Constant compressibility of gas over each pipe.

- Constant friction coefficient along each pipe.
- Darcy friction loss across a pipe is valid.

For the model the derivation as described in Osiadacz [1987] is followed, and the links are assumed to represent pipelines and not compressors or valves. First, Kirchhoff's first law is used, which states that sum of all flows entering and leaving a node through a pipe must be equal to the flow entering a leaving a node due to a load:

$$L = A'q \quad (1)$$

where L is the $(N - 1) \times 1$ vector of loads, i.e. gas demands, at each node, A' is the $(N - 1) \times N_e$ reduced branch-nodal incidence matrix, where N_e is the number of edges and q is the $N_e \times 1$ vector of gas flow along each edge. The branch-nodal incidence matrix A is defined by:

$$A = \begin{cases} 1, & \text{if the flow of a pipe enters the node} \\ -1, & \text{if the flow of a pipe leaves the node} \\ 0, & \text{otherwise} \end{cases} \quad (2)$$

To obtain the reduced branch-nodal incidence matrix A' , the row for the slack node is removed from A . Then, Kirchhoff's second law is used, which states that the pressure drop over each closed loop must be zero:

$$B\Delta p = 0 \quad (3)$$

where B is the $N_{\text{loops}} \times N_e$ branch-loop incidence matrix and Δp is the $N_e \times 1$ vector of pressure drops over each edge given by:

$$\Delta p = -A^T p \quad (4)$$

with A^T the transpose of the branch-nodal incidence matrix and p the $N \times 1$ vector of nodal pressures.

A steady-state flow equation is used to give the relation between the gas flow q and the pressure drop Δp . There are multiple formulations possible for the steady-state flow equation, e.g. Lacey's equation for low pressure, Polyflo equation for medium pressure, or Weymouth equation for high pressure. A commonly used steady-state flow equation for horizontal pipes is given by:

$$(q_n)_k = S_{ij} \left(\frac{S_{ij}(p_i^2 - p_j^2)}{K_k} \right)^{\frac{1}{m}} \quad (5)$$

where $[\cdot]_n$ is used to refer to the value $[\cdot]$ at standard pressure, k is the pipe index for the pipe between nodes i and j , K is the pipe constant which depends on the friction coefficient of the pipe,

$$S_{ij} = \begin{cases} 1, & \text{if } p_i > p_j \\ -1, & \text{if } p_i < p_j \end{cases} \quad (6)$$

and m is a factor which is 2 for low pressures (0-100mbar), 1.848 for medium pressures (0.1-7bar) and 1.854 for high pressure networks [Abeysekera, 2016], [Osiadacz, 1987].

We present three ways to solve for the pressures p at the nodes and the gas flow q in the pipes, namely nodal formulation, loop formulation and the nodal-loop formulation.

Nodal formulation For the nodal formulation the pressure at the nodes are taken as unknowns. Again, the first step is Kirchhoff's first law. However, the vector q consists of the flows at the edges. Therefore, the steady-state flow equation is used to express the flow q as a function of the pressure drops Δp . Since there are multiple versions of the steady-state flow equation, this relation is kept general:

$$q = \phi^{-1}(\Delta p) \quad (7)$$

Substituting this in Kirchhoff's first law gives:

$$L = A' \phi^{-1}(\Delta p) = A'[\phi^{-1}(-A^T p)] \quad (8)$$

This can be rewritten as a nonlinear function of the nodal pressure:

$$F(p) = L - A'[\phi^{-1}(-A^T p)] \quad (9)$$

and the nodal pressures p can be found by solving the non-linear system of equations $F = 0$, for which for instance Newton-Raphson (NR) can be used. After the nodal pressures are determined, the steady-state flow equation can be used to compute the gas flows on each edge. Note that this system of non-linear equations corresponds to the mismatch function used in the steady-state analysis of power grids.

When using NR to solve the non-linear system of equations, the Jacobian matrix $J = \frac{\partial(F)}{\partial p}$ is used. Assuming the commonly used equation for low pressure flow (5) it holds that:

$$\frac{\partial q_{ij}}{\partial p_i} = \frac{2}{m} \frac{p_i}{p_i^2 - p_j^2} q_{ij} \quad (10)$$

$$\frac{\partial q_{ij}}{\partial p_j} = \frac{-2}{m} \frac{p_j}{p_i^2 - p_j^2} q_{ij} \quad (11)$$

The Jacobian matrix J is then given by:

$$J = -A' D A^T \quad (12)$$

with

$$D = \text{diag} \left(\frac{2}{m} \frac{p_k}{\Delta p_k^2} q_k \right) \quad (13)$$

where k denotes the edge between node i and j and $\Delta p_k^2 := p_i^2 - p_j^2$. For the nodal formulation the Jacobian matrix is sparse and relatively simple [Wobbes, 2015]. However, NR for the nodal formulation shows poor convergence behavior and is sensitive to initial values. Also note that if the nodal pressures are initialized incorrectly (i.e. if all nodal pressures are initialized with the same value such that $\Delta p = 0$), the Jacobian matrix becomes singular.

Loop formulation Another way to perform the steady-state analysis of the gas network is by using the loop formulation. This formulation takes the gas flow on each edge as unknowns. The starting point of the loop formulation is Kirchhoff's second law which uses the vector Δp of pressure drops over each edge. To express the the pressure drops in terms of the gas flow the steady-state flow equation (7) is used:

$$\Delta p = \phi(q) \quad (14)$$

Substituting this in Kirchhoff's second law gives:

$$B\phi(q) = 0 \quad (15)$$

Kirchhoff's second law ensures that the pressure drops over a loop sum up to zero. In order to ensure that Kirchhoff's first law is obeyed, an initial approximation for the edge flows q^0 is made. Then, the true edge flows q are determined using correction term called the loop flow q^{loop} , which is a vector of length N_{loops} . This correction is added to or subtracted from the initial approximation based on the direction of the flow within a loop:

$$q = q^0 + B^T q^{\text{loop}} \quad (16)$$

Substituting this in equation (15) results in the following system of equations:

$$F(q^{\text{loop}}) = B\phi(q^0 + B^T q^{\text{loop}}) = 0 \quad (17)$$

This is a system of non-linear equation which can be used to solve for the loop flow q^{loop} for each loop. After the loop flows are used to determine the gas flows q , the steady-state flow equation can be used to determine the nodal pressures. Newton-Raphson can be used to solve the non-linear system of equations. Assuming the commonly used equation for low pressure flow (5) it holds that:

$$\frac{\partial F(q^{\text{loop}})}{\partial q^{\text{loop}}} = K_k m (S_k q_k)^{m-1} = K_k m |q_k|^{m-1} \quad (18)$$

where the last equality holds because S_k and q_k always have the same sign. The Jacobian matrix is then given by:

$$J = BMB^T \quad (19)$$

with

$$M = \text{diag}(mK_k |q_k|^{m-1}) \quad (20)$$

For the loop formulation the Jacobian matrix is square, symmetric and has positive diagonal elements. NR also shows good convergence behavior for the loop formulations [Wobbes, 2015]. The downside of the loop formulation is that the network has to be divided into loops in order to determine matrix B .

Nodal-loop formulation The third way to perform the steady-state analysis of the gas network is the nodal-loop formulation. This formulation combines the nodal and loop formulation in order to use the sparseness of the nodal formulation and the convergence behavior of the loop formulation. Like the loop formulation, the nodal-loop formulation solves the loop pressure equation $B\phi(q) = 0$. But instead of solving this system for the gas flows, the loop pressure equation is rewritten to nodal equations using a first order Taylor expansion for $\phi(q)$, which results in the following system [Osiaacz, 1987]:

$$J^k p_1^{k+1} = A_1 (R^k)^{-1} (\Delta p^k + A_2^T p_2) \quad (21)$$

where k is the iteration index, J is the Jacobian, $R = \frac{\partial \phi(q)}{\partial q}$ resulting from the Taylor expansion, A_1 is the branch-nodal incidence matrix for unknown pressures, A_2 is the branch-nodal incidence matrix for known pressures, p_1 is a vector of unknown nodal pressures and p_2 is a vector of known nodal pressures. This equation is solved to obtain the unknown nodal pressures p_1 .

Note that the Jacobian is an $N_L \times N_L$ matrix, where N_L is the number of load nodes. Furthermore, the following holds for the Jacobian. Let k denote a link between nodes i and j . A diagonal entry in J corresponds to a particular load node, and consist of the sum of R_k^{-1} for all links k connected to that particular node. An off-diagonal entry in J corresponds to a connection between two load nodes and is given by R_k^{-1} where k is the link that connects these two load nodes. Assuming the commonly used equation for low pressure flow (5), R_k^{-1} is given by:

$$R_k^{-1} = \frac{1}{mK_k|q_k|^{m-1}} \quad (22)$$

2.1.4 Components

Recall that in the derivation of all three formulations above a network without valves or compressors was assumed. However, in practice, most gas networks will contain both valves and compressors. Therefore, these two components are described in more detail in this section.

Valve Valves are used to regulate the flow and the pressure within a network. They are active components, meaning that they are controlled by an operator. There are valves that can be controlled remotely (automated), or valves that need to be physically operated (non-automated). The most commonly used type of valves is a gate valve or a ball valve [Koch et al., 2015]. The gate valve is controlled by lowering or dropping a gate wall. The ball valve consist of a ball with a cylinder cut out in the middle. If this cylinder is aligned with the pipe lines, the valve is completely open. If the ball is rotated by 90 degrees, such that the cylinder does not align with the pipe lines, the valve is completely closed. Other types of valves that can be used to control the flow are plug and butterfly valves [Osiaadacz, 1987]. Note that valves are generally small, such that the friction over a valve can be neglected.

Check valves can be used to prevent back flow in pipe lines [Osiaadacz, 1987]. They are kept open by the flow of the gas and are closed when the direction of flow is reversed.

Finally, valves can also be used as control valves or pressure regulators, which are used to regulate the pressure between parts of the network operating at different pressures, e.g. between the transportation and the distribution grid [Koch et al., 2015].

Compressor Compressors compress the flowing gas and thereby increase the pressure. This is used to overcome pressure losses or to transport gas over long distances. Compressors are generally driven by one of four types of drive, namely by gas turbines, gas motors, electric motors, or steam turbines [Koch et al., 2015]. The compressor types used most often are generally either a turbo compressor or a piston compressor.

In practice every compressor has a feasible operating range, which is the set of possible combinations of throughput, which is measured in volumetric flow, and specific change in adiabatic enthalpy [Koch et al., 2015]. Assuming that the compression is adiabatic, i.e. no heat exchange with the surroundings, and assuming that the gas can be seen as an ideal gas, the following holds for the enthalpy \tilde{H} :

$$\tilde{H} = p_{in}V_{in} \frac{x}{x-1} \left[\left(\frac{p_{out}}{p_{in}} \right)^{\frac{x-1}{x}} - 1 \right] \quad (23)$$

where p_{in} and p_{out} are the inflow and outflow pressure respectively, V_{in} is the inlet volume and x is the isentropic exponent. Using the ideal gas law $p_{in}V_{in} = nRT_{in}$, with n the amount of gas (in

moles), R the gas constant and T_{in} the inlet temperature, the equation for the change in enthalpy can be rewritten to:

$$\tilde{H} = nRT_{in} \frac{x}{x-1} \left[\left(\frac{p_{out}}{p_{in}} \right)^{\frac{x-1}{x}} - 1 \right] \quad (24)$$

To make this independent of the amount of gas (i.e. independent of n), the change in enthalpy \tilde{H} is divided by the molar mass M . Using $n = \frac{m}{M}$, with m the mass, results in the change in specific adiabatic enthalpy:

$$H = R_s T_{in} \frac{x}{x-1} \left[\left(\frac{p_{out}}{p_{in}} \right)^{\frac{x-1}{x}} - 1 \right] \quad (25)$$

where $R_s = \frac{R}{M}$ is used to denote the specific gas constant and $H := \frac{\tilde{H}}{M}$ is the specific enthalpy. The power P required for the compression of gas depends on the enthalpy, on the amount of gas compressed measured in mass flow q_{mass} and on the adiabatic efficiency η :

$$P = \frac{q_{\text{mass}} H}{\eta} \quad (26)$$

Note that the compression of gas heats the gas, such that in practice some cooling technique is applied at the outlet of the compressor.

The general approach above holds for both turbo and piston compressors even though they compress the gas using a different technique. Turbo compressors compress the gas by rotation, meaning that the required energy for compression depends on the rotation speed. Piston compressors compress the gas by using a crankshaft. In general, turbo compressors can compress larger amounts of gas whereas piston compressors can compress the gas more although only for smaller amounts of gas. For instance, the compressor ratio for a turbo compressor are typically between 1.35 to 1.5 whereas for a piston compressor the ratio can go up to 4 [Koch et al., 2015]. The typical maximum power required varies between 5 MW and 25 MW.

For gas-driven compression, the energy required to operate the compressor is taken from the gas network itself. The gas is taken from the inlet of the compressor and therefore has the same pressure as the gas flow coming in to the compressor. The required amount of gas τ_{ij} for a compressor between nodes i and j is usually determined using a quadratic polynomial (e.g. An et al. [2003], Martinez-Mares and Fuerte-Esquivel [2012], or Shabanpour-Haghighi and Seifi [2016]):

$$\tau_{ij} = \alpha_{ij} + \beta_{ij} P_{ij} + \gamma_{ij} P_{ij}^2 \quad (27)$$

where P_{ij} is the power required by the compressor between nodes i and j , see equation (26), and α_{ij} , β_{ij} , and γ_{ij} are the compressor consumption coefficients.

If the compressor is driven by an electric motor the following relation between required active power P^a (see section on electrical network for explanation on active power) and power required by the compressor P_{ij}^{hp} measured in horse power is commonly used (e.g. Shabanpour-Haghighi and Seifi [2016], Martinez-Mares and Fuerte-Esquivel [2012]):

$$P^a = \frac{745.7 \cdot 10^{-6}}{3600} P_{ij}^{\text{hp}} \quad (28)$$

where P^a is measured in MW.

2.2 Electricity

2.2.1 Physical power grid

Schavemaker and Van der Sluis [2008] describe the physical power grid. A summary is given below. The total power system consist of generation, transmission and distribution of (electrical) power. Power is transported by overhead or underground transmission lines. The design of the transmission lines is determined by the required power and the distance over which the power has to be transported. In general the greater the distance and the more power that has to be transported, the higher the voltage across a transmission line. This means that the voltage of the transmission grid is higher than the voltage of the distribution grid. See Figure 2 for a schematic representation of the power system. For the Netherlands, the transmission grid can be subdivided into two parts,

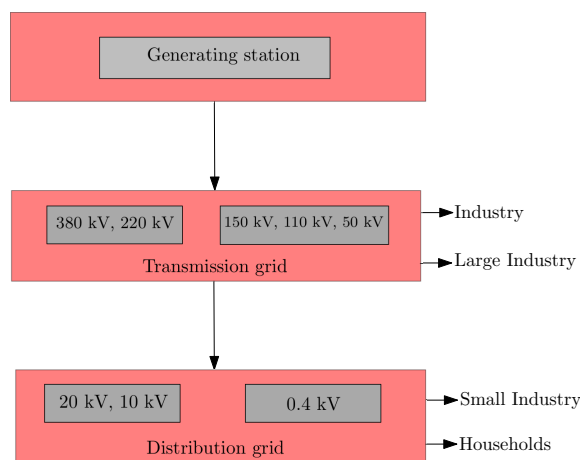


Figure 2: Schematic representation of the power grid. The voltage levels are typical to the Dutch network.

one with voltages of 380 kV and 220 kV, and one part of 150 kV, 110 kV or 50 kV. The second part with the lower voltages is sometimes also called the sub-transmission networks. The distribution grid can also be subdivided into two parts, one with voltages of 20 kV and 10 kV and one part 0.4 kV.

The power grid can be considered steady-state. In the Netherlands, AC current alternates at 50 Hz, which is equivalent to a wavelength of 6000 km. Since the transmission lines (both in the transmission grid and the distribution grid) are small compared to this length, a steady-state approximation can be used, which means that Kirchoff's law can be used. The frequency is assumed to be constant in steady-state analysis. This means that voltage and current can be represented by a phasor, which only contains information about angle and amplitude (i.e. frequency is not included in this phasor representation).

Usually, in reality, both the transmission and distribution system are three-phase systems. If the three-phase system is balanced, the voltages have the same magnitude and their angles are shifted by 120° . Furthermore, the instantaneous power is constant in a balanced three-phase system, as opposed to in the single-phase system where the instantaneous power varies in time with double

the power frequency. When solving a balanced three-phase system, the system can be approximated with a single-phase system equivalent to the three-phase system. From now on, a balanced three-phase AC system will be assumed.

2.2.2 Network representation

When representing the power grid as a network, nodes and links are introduced. The nodes are generally called busses in a power grid. They represent any point in the grid in which power enters or leaves the network (sources or loads), or any point in the grid where the power is simply redistributed. The representation of the power grid as a network follows the representation as described by Schavemaker and Van der Sluis [2008]. A bus is fully described (electrically) by four parameters:

- the voltage magnitude $|V|$
- the voltage angle δ
- the injected active power P
- the injected reactive power Q

Generally, three types of busses are distinguished and only two of the four parameters are known for each bus, see Table 2. In more detail, the following can be said about the node types:

Table 2: Node types for power grid

Node type	Number of nodes	Specified parameters	Unknown parameters
slack node	1	$ V_i , \delta_i$	P_i, Q_i
generator bus (PV-bus)	N_g	$P_i, V_i $	Q_i, δ_i
load bus (PQ-bus)	$N - N_g - 1 := N_L$	P_i, Q_i	$ V_i , \delta_i$

- Load bus: In power flow analysis, loads can be modeled statically or dynamically. When computing the solution to the load flow problem, static loads are used. Still, multiple ways of modeling loads exists [Sereeter et al., 2016]. Loads are usually modeled as constant power sinks (constant power load) instead of impedances [Schavemaker and Van der Sluis, 2008]. Since steady-state power flow analysis is considered, the active and reactive power are assumed to be known and constant.
- Generator bus: A bus through which power can enter the network. In practice the active power and the voltage angle can be controlled at a generator and are therefore assumed to be known.
- Slack node: For the load flow computation to be well defined, a reference node for the voltage is needed. This node serves as reference for the other nodes, which means that the voltage angle and amplitude are specified. The actual value of the voltage angle is not important since the voltage angle of all the other nodes is only calculated with respect to the reference angle (i.e. only angle differences are determined). The slack node ensure that enough power is supplied to the network to meet all the demands. Generally, the slack node and the reference node are taken to be the same node, which is usually a generator.

Note that even though a wind turbine usually provides power to the grid, it is not modeled as a generator but as a load since it does not have the active power and voltage amplitude as control. Nodes that only redistribute the power, i.e. where no load or generator is connected, are modeled as load nodes with injected active and reactive power set to zero (i.e. $P = Q = 0$). A node that has both a load and a generator connected to it are modeled as a generator bus with $|V| = |V|_{gen}$ and $P = P_{gen} + P_{load}$

The links in the network represent the transmission lines in the grid. For a transmission line, four parameters can be distinguished:

- the series resistance, which is due to the resistivity of the conductor.
- the inductance, which is due to the magnetic field surrounding the conductor.
- the capacitance, which is due to the electric field between the conductors.
- the shunt conductance, which is due to the leakage currents in the insulation.

For a long transmission line (> 240 km), the length of the line has to be taken into account for the derivation of the equivalent circuit (or network representation). Since the main interest is with the distribution grid, these long lines will not be considered.

For a medium transmission line (approximately between 80 km and 240 km) the equivalent circuit representation is given in Figure 3. The equivalent circuit of the medium-length transmission line is made up of the total series impedance z of the transmission line with half of the total shunt capacitance y^{sh} at each side of the line.

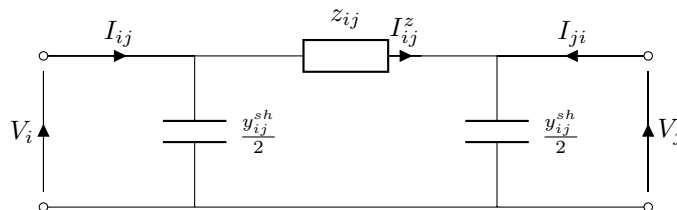


Figure 3: Equivalent circuit medium length transmission line

For a short transmission line (< 80 km) the equivalent circuit is given in Figure 4. The equivalent circuit of the short transmission line takes only the the total series impedance of the transmission line into account.

As mentioned before, the links in the graph representation of the power grid correspond to the transmission line. In case of medium length transmission line a link will therefore also include the shunts. Even though the current I can be seen as equivalent to the gas flow q (see Section 3) the inclusion of the shunts means that $I_{ij} \neq I_{ji}$, which can be seen from Figure 3.

2.2.3 Model

The derivation of the models follows the derivation of the model as described in Schavemaker and Van der Sluis [2008] and Idema [2012]. Before the power flow (or load flow) problem can be solved, the relations and models of the underlying quantities (relating to power) are needed. To understand

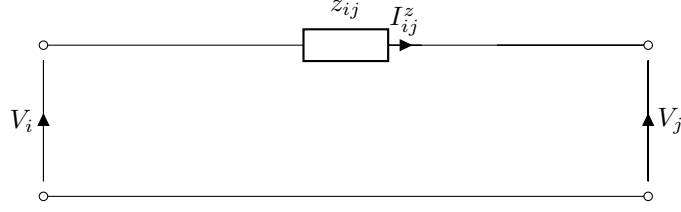


Figure 4: Equivalent circuit short length transmission line

these underlying models, a single-phase circuit will be looked at. Recall that in the steady-state approach the frequency is assumed to be constant, meaning that the voltage V and current I can be represented by their effective phasor:

$$V = |V|e^{\iota\delta_V}$$

$$I = |I|e^{\iota\delta_I}$$

where $|V|$ and $|I|$ are the absolute value, δ_V and δ_I are the angle of the voltage and current respectively and ι is the imaginary unit. Note that $|V|$ and $|I|$ are the RMS value of $v(t)$ and $i(t)$, which are the voltage and current as used in circuit theory. This means that $|V| = \frac{V_{max}}{\sqrt{2}}$ and $|I| = \frac{I_{max}}{\sqrt{2}}$, or, in other words, the effective phasor differs a factor $\sqrt{2}$ from the circuit theory phasor. The relation between current and voltage for the common circuit elements is shown in Table 3. Looking at a single-phase circuit, see Figure 5, and using that $v(t) = \sqrt{2}|V| \cos(\omega t)$ and

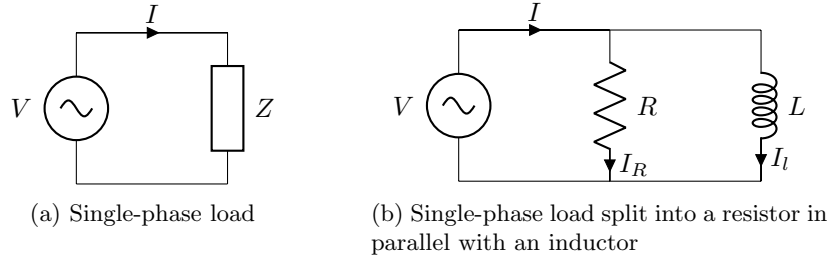


Figure 5: Single-phase circuit

$i(t) = \sqrt{2}|I|\cos(\omega t - \phi)$ the instantaneous power $p(t)$ consumed by impedance Z is given by:

$$p(t) = 2|V||I| \cos(\omega t) \cos(\omega t - \phi)$$

$$= |V||I| \cos(\phi) [1 + \cos(2\omega t)] + |V||I| \sin(\phi) \sin(2\omega t)$$

$$:= P [1 + \cos(2\omega t)] + Q \sin(2\omega t)$$

where ϕ is the phase shift between voltage and current, i.e. ϕ is positive for a current lagging the voltage and negative for a leading current. And where ω is the frequency. The first term ($P [1 + \cos(2\omega t)]$) describes an unidirectional component of the instantaneous power with an average value P . This value P is called the average, real or active power and has unit Watt [W]. The second term ($Q \sin(2\omega t)$) is alternately positive and negative and has an average value of zero. This term

Table 3: Circuit elements (Wolfson [2007], Schavemaker and Van der Sluis [2008])

Circuit Element	Current vs voltage	Peak current vs peak voltage	Phase relation	Explanation
Resistor	$I = \frac{V_p}{R} \sin \omega t$	$I_p = \frac{V_p}{R}$	V and I in phase	An ideal resistor is a device whose current and voltage are always proportional.
Capacitor	$I = \omega C V_p \sin(\omega t + \frac{\pi}{2})$	$I_p = \frac{V_p}{1/\omega C} := \frac{V_p}{X_C}$	I leads V by 90°	Current leads voltage because the capacitor voltage is proportional to its charge, and it takes current to move charge onto the capacitor plates.
Inductor	$I = \frac{V_p}{\omega L} \sin(\omega t - \frac{\pi}{2})$	$I_p = \frac{V_p}{\omega L} := \frac{V_p}{X_L}$	V leads I by 90°	Voltage leads current because a changing current in an inductor induces an electromagnetic force. Before the current can build up significantly, there must first be voltage across the inductor

describes a bidirectional component of the instantaneous power. When this term has a positive sign, the power flow is towards the load; when the sign is negative, the power flows from the load back to the source. Because the average value of this oscillating power component equals zero, it gives on average no transfer of energy towards the load. The amplitude Q of this oscillating power is called imaginary or reactive power, which has as unit reactive voltamperes [var]. From the instantaneous power $p(t)$ it can be found that the following holds for P and Q :

$$P = |V||I| \cos(\phi)$$

$$Q = |V||I| \sin(\phi)$$

Furthermore, $\cos(\phi)$ is called the power factor. When looking at a load as in Figure 5b (i.e. modeling an inductive load as a resistor in parallel with an inductor), the first term ($P [1 + \cos(2\omega t)]$) corresponds to the instantaneous power consumed by the resistor, and the second term ($Q \sin(2\omega t)$) corresponds to the instantaneous power towards the conductor. Therefore, a part (VI_R) of the instantaneous power $p(t)$ consumed by an element is utilized for permanent consumption, such as conversion into heat. This part always has a positive value, i.e. it cannot be returned to the rest of the circuit. The other part of $p(t)$ (VI_L) is used to establish either a magnetic or electric field. This means that it is taken from and returned to the circuit with double the power frequency (due to the 2ω in $Q \sin(2\omega t)$).

Complex power S in voltampere [VA] is defined as:

$$S := VI^* = P + \iota Q$$

where $[\cdot]^*$ is used to denote the complex conjugate. This definition is chosen such that the reactive power has the right sign, i.e. such that an inductive load (where the current lags the voltage)

consumes reactive power. The apparent power $|S|$ is then defined as:

$$|S| := |V||I| = \sqrt{P^2 + Q^2}$$

Note that reactive voltampere [var] and voltampere [VA] are the same unit as watt [W], but the different terminologies are used to be able to make a distinction between reactive power, complex power and active power.

Now that the relations of the underlying electrical quantities are known, the steady-state power flow problem can be solved. The formulation of the load flow problem that is commonly used starts with Ohm's law:

$$I = YV$$

where I is a vector of length N of injected currents at each node, with N the total number of nodes. V is a vector of length N of node voltages and Y is the admittance matrix. To obtain the admittance matrix, Kirchhoff's current law is used, which gives that Y_{ii} is the sum of all admittances directly connected to node i and Y_{ij} is the negative value of total admittance connected between node i and node j . Note that $Y_{ij} = Y_{ji}$. The equations obtained using Kirchhoff's current law are nodal equations.

Expressions for the power flow can be obtained by substituting Ohm's law in the expression for complex power:

$$\begin{aligned} S_i &= V_i I_i^* = V_i (YV)_i^* \\ &= V_i \sum_{k=1}^N Y_{ik}^* V_k^* \\ &= \sum_{k=1}^N |V_i||V_k| (\cos(\delta_{ik}) + \iota \sin(\delta_{ik})) (G_{ik} - \iota B_{ik}) \end{aligned} \quad (29)$$

where S_i is the injected complex power at node i , I_i is the current through node i , i.e. the sum of all currents entering and leaving node i , V_i is the node voltage, N is the total number of nodes and $\delta_{ij} = \delta_i - \delta_j$ is the difference between voltage angles. G_{ij} and B_{ij} are respectively the conductance and susceptance over the link between node i and node j . Note that the power flow problem (29) is a nonlinear system of equations.

To formulate the power flow problem in terms of active and reactive power, note that $S_i = P_i + \iota Q_i$, which gives:

$$\begin{aligned} P_i &= \sum_{k=1}^N P_{ik} \\ Q_i &= \sum_{k=1}^N Q_{ik} \end{aligned}$$

where P_i and Q_i are injected active and reactive power respectively, and:

$$P_{ij} = \begin{cases} |V_i||V_j| (G_{ij} \cos(\delta_{ij}) + B_{ij} \sin(\delta_{ij})), & \text{if node } j \text{ is connected to node } i \\ 0, & \text{if node } j \text{ is not connected to node } i \end{cases} \quad (30)$$

$$Q_{ij} = \begin{cases} |V_i||V_j| (G_{ij} \sin(\delta_{ij}) - B_{ij} \cos(\delta_{ij})), & \text{if node } j \text{ is connected to node } i \\ 0, & \text{if node } j \text{ is not connected to node } i \end{cases} \quad (31)$$

Using this, a power mismatch function can be defined:

$$\Delta F(x) = \begin{pmatrix} P^{spec} - P^{comp} \\ Q^{spec} - Q^{comp} \end{pmatrix} \quad (32)$$

Where P^{spec} and Q^{spec} are the specified (i.e. known) active and reactive power injected in the nodes, P^{comp} and Q^{comp} are the vectors of length N consisting of the P_i 's and Q_i 's, meaning that $\Delta F(x)$ has length $2N$ and x is a vector of length $2N$ defined as:

$$x = \begin{pmatrix} \delta_1 \\ \vdots \\ \delta_N \\ |V_1| \\ \vdots \\ |V_N| \end{pmatrix}$$

The power flow equations are then given by $\Delta F(x) = 0$, which leads to an $2N$ system of non-linear equations. This system can be solved using Newton-Raphson with Jacobian matrix given by:

$$J = \frac{\partial(\Delta F)}{\partial x} = - \begin{pmatrix} \frac{\partial(\Delta P)}{\partial \delta} & \frac{\partial(\Delta P)}{\partial |V|} \\ \frac{\partial(\Delta Q)}{\partial \delta} & \frac{\partial(\Delta Q)}{\partial |V|} \end{pmatrix} \quad (33)$$

First note that from equation for the active (30) and reactive power (31) it can be concluded that:

$$P_{ii} = |V_i|^2 G_{ii} \quad (34)$$

$$Q_{ii} = -|V_i|^2 B_{ii} \quad (35)$$

This means that the following holds for the elements of the Jacobian:

$$\begin{aligned}
\frac{\partial P_i}{\partial \delta_i} &= -Q_i - |V_i|^2 B_{ii} \\
\frac{\partial P_i}{\partial \delta_j} &= Q_{ij} \\
\frac{\partial Q_i}{\partial \delta_i} &= P_i - |V_i|^2 G_{ii} \\
\frac{\partial Q_i}{\partial \delta_j} &= -P_{ij} \\
\frac{\partial P_i}{\partial |V|_i} &= \frac{P_i + |V_i|^2 G_{ii}}{|V_i|} \\
\frac{\partial P_i}{\partial |V|_j} &= \frac{P_{ij}}{|V_j|} \\
\frac{\partial Q_i}{\partial |V|_i} &= \frac{Q_i - |V_i|^2 B_{ii}}{|V_i|} \\
\frac{\partial Q_i}{\partial |V|_j} &= \frac{Q_{ij}}{|V_j|}
\end{aligned}$$

In the Jacobian, the equations (i.e. rows) corresponding to nodes for which P or Q are unknown, such that P^{spec} or Q^{spec} are unknown, are not taken into account. Looking at Table 2, it can be seen that 2 equations (1 for P and 1 for Q) are removed for the slack node and 1 equation (for Q) is removed for each generator node. Therefore, there is a total of $2N - 2 - N_g$ equations left. Similarly, for some nodes $|V|$ or δ are known, and these values can be removed from x (i.e. columns can be removed from $\Delta F(x)$). Looking at Table 2, it can be seen that 2 columns (one for $|V|$ and one for δ) are removed for the slack node and 1 column (for $|V|$) is removed for each generator node. This means that there are $2N - 2 - N_g$ columns left. Note that this is equal to $N_g + 2N_L$, which can also be seen from Table 2, since each load node has 2 unknown variables (both $|V|$ and δ) and at the same time allows for 2 equations (since both P and Q are known). Similarly a generator node has 1 unknown variable (δ) and at the same time allows for 1 equation (since only P is known). Therefore, the resulting system consists of $2N_L + N_g = 2N - N_g - 2$ non-linear equations and $2N_L + N_g = 2N - N_g - 2$ variables. These are nodal equations with two equations per load node and one equation per generator node.

The method described above is the most common used formulation of the mismatch function for the load flow problem, since it is considered to result in the best convergence behavior and robustness when using Newton-Rapshon. It is, however, possible to formulate the mismatch equation in other ways. An overview and comparison of these other formulations is given in Sereeter et al. [2016]. The formulation described above uses the power mismatch function and polar coordinates. After eliminating the reactive power mismatch ΔQ and ΔV for each PV bus this results in a system with $2N - 2 - N_g$ equations. A second option is to use the power mismatch function and Cartesian coordinates. In this case, the reactive power mismatch ΔQ is replaced with the voltage-magnitude-squared mismatch $\Delta |V|^2$ for each PV bus. This results in a system with $2N - 2$ equations, i.e. a number of equations equal to the number of PV buses more than for the polar coordinates. This formulation of the mismatch function is slightly less reliable and results in slightly slower convergence

than the formulation with power mismatch and polar coordinates. After improvements, Sereeter et al. [2016] reduces the system to $2N - N_g - 2$ equations, which is the same amount of equations as the formulation using power mismatch and polar coordinates. As a third option, the load flow problem can be formulated using the power mismatch and complex coordinates. This results in a system with $N - 1$ equations. A fourth option is to formulate the load flow problem using the current mismatch function and polar coordinates. Each PQ bus is represented by two equations derived from the complex current mismatch function. Each PV bus is represented by one equation for the active power mismatch ΔP and one equation for the voltage-magnitude-squared mismatch $\Delta|V|^2$. This results in a system with $2N - 2$ equations. This formulation performs worse than the power mismatch formulation. As a fifth option the load flow problem can be formulated using the current mismatch and Cartesian coordinates. This requires the introduction of ΔQ as a dependent variable for each PV bus (instead of the real part of the voltage $\text{Re}\{\Delta V\}$). The real and imaginary current mismatch functions are expressed in terms of P^{spec} and Q^{spec} and in terms of the real and imaginary part of the voltage. This leads to a system with $2N - 2$ equations. The sixth and final formulation of the load flow problem uses the current mismatch function and complex coordinates. This leads to a system of $N - 1$ equations. After the improvements by Sereeter et al. [2016] the formulations using the current-mismatch functions shows better convergence for a distribution network than the formulations using the power-mismatch, regardless of the coordinates chosen.

2.2.4 Power loss

Another important quantity in power grids is the power loss over a line or component. First note that P_{ij} and Q_{ij} are not edge variables, moreover $P_{ij} \neq P_{ji}$ and $Q_{ij} \neq Q_{ji}$. Power loss, on the other hand, is an edge variable and for a link between node i and j it is given by:

$$P_{ij}^{\text{loss}} = P_{ij} + P_{ji} \quad (36)$$

$$Q_{ij}^{\text{loss}} = Q_{ij} + Q_{ji} \quad (37)$$

Depending on whether the link is representing a medium length or a short length transmission line (see Figures 3 and 4) the reactive power loss is the power loss over the impedance and the power loss due to the shunts, or only the power loss over the impedance.

Another way to calculate the power loss over the impedance between nodes i and j is to use the definition of the complex power [Idema, 2012]:

$$S_{ij}^{z,\text{loss}} = (I_{ij}^z)^* \Delta V_{ij} \quad (38)$$

Note that the real part of $S_{ij}^{z,\text{loss}}$ corresponds to the active power loss over the impedance and the imaginary part of $S_{ij}^{z,\text{loss}}$ corresponds to the reactive power loss over the impedance.

2.2.5 Distributed slack node approach

In the derivation of the non-linear system of equations for the power flow (32) the commonly used classification of nodes as given in Table 2 was assumed. In this classification there is only one slack node, which also functions as a reference node. However, it is possible to have more than one node function as a slack node. This is called the distributed slack node approach. It was first introduced by Guoyu [1985], and later used for load-flow computations by Exposito et al. [2004] in a power grid and by Martinez-Mares and Fuerte-Esquivel [2012] and Shabanpour-Haghighi and Seifi

[2016] for integrated systems. In order to have multiple nodes function as slack nodes, an unknown participation factor β is introduced for every potential slack node. Then the imbalance ΔP^{gen} between the specified active power generation and the active power demands plus transmission losses is distributed over all possible slack nodes according to the participation factors. This means that for every potential slack node the injected active power is given by a combination of a specified set-point and a part of the generation imbalance, instead of being fully specified:

$$P_i^{\text{gen}} = P_i^{\text{gen}0} + \beta_i \Delta P^{\text{gen}} \quad (39)$$

where P_i^{gen} is the active power injected into the network by the slack node, $P_i^{\text{gen}0}$ is the specified set-point of the generator and β_i is the participation factor of the slack node. The participation factors are normalized, i.e. $\sum_i^{N_g} \beta_i = 1$.

Note that following relations hold:

$$\sum_i^{N_g} P_i^{\text{gen}} = \sum_j^{N_L} P_j^{\text{spec}} + \sum_k P_k^{\text{loss}} = \sum_i P_i^{\text{gen}0} + \Delta P^{\text{gen}} \quad (40)$$

where P_k^{loss} is the active power transmission loss over link k and P_j^{spec} is the specified active power demand for load node j . Furthermore, note that there must still be (at least) one reference node to fix the voltage amplitude and voltage angle.

The distributed slack node approach introduces $N_g - 1$ extra unknowns, in the form of the participation factors β , to the system of non-linear equations.

2.3 Heat

2.3.1 District Heating

A district heating network generally consists of a return and supply line. The supply line transports hot water or steam from the source to the loads. After the loads extract heat, the cold water is transported back to the source by the return line to be heated up again. See also Figure 6. In the Netherlands, the conventional systems operate at 120° at the source and 90° at the entry of a load. Newer networks have lower supply temperatures, but at least 70° is required at the entry of a load in order to be able to use hot tap water [van Economische zaken, Landbouw en Innovatie]. On the other hand, Frederiksen and Werner [2013] state that 55° is a typical temperature for hot tap water, since it is warm enough to ensure hygiene and to prevent Legionella and cold enough to prevent the burning of skin.

The heating system is a closed loop system and can be used to provide heat or hot water to a load. In the Netherlands district heating is applied on different scales, e.g. for a city ('stadsverwarming') or on a smaller scale for a block of houses ('blokverwarming'). In Sweden, the average pipe diameter for a district heating system is 0.14 m, the wider pipes have an average diameter of 0.20-0.25 m and the pipes in a sparse area have an average pipe diameter of 0.03-0.05 m [Frederiksen and Werner, 2013].

Generally, two types of heating networks can be distinguished; a traditional network, which is sometimes also called a Y-network, or a ring network [Kuosa et al., 2013]. In a Y-network, each splitting of pipes is a Y-splitting, i.e. each splitting consists of three pipes, see Figure 7a. The

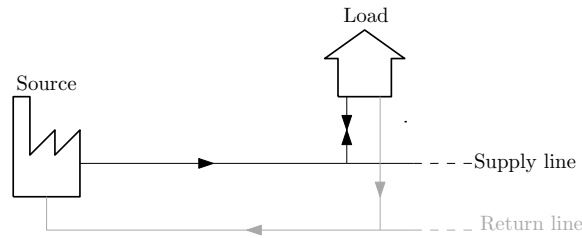


Figure 6: Example of a source and load connected to a supply (black) and return (grey) line.

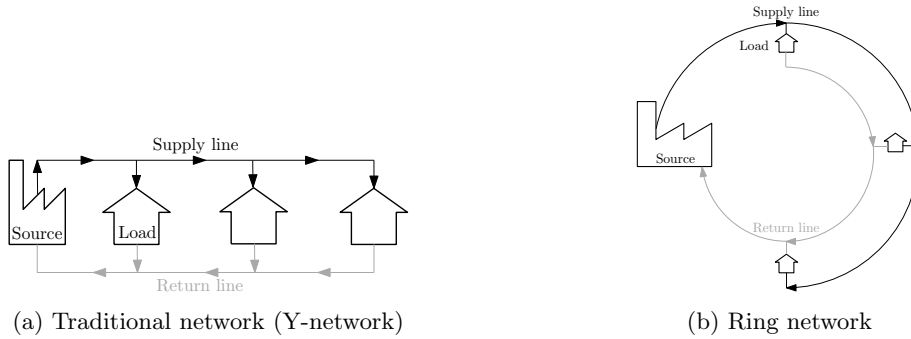


Figure 7: Two types of heating networks

temperature of the water at the source is determined by the outside temperature and the flow to the loads is controlled using valves. Note that the partial network shown in Figure 6 also shows a Y-network. The advantage of a Y-network is that it is easy to construct. The downside is that the pipe length (supply and return line added together) between source and the different loads varies. Water tends to follow the shortest possible route, which would be through the first consumer. To prevent this, the valves at the first consumer are closed the most, resulting in large local pressure differences and losses. Furthermore, such a network is slow to control. Finally, the main pump must be able to cope with the pressure difference between the source and the load furthest from the source.

In a ring-network, the loads are connected to the supply and return line in a ring, see Figure 7b. The loads are connected to network using pumps, which are driven by the heat demand of the load and by the required return temperature. The first advantage of the ring network is these pumps, meaning that a ring network is especially suitable for mass flow control. Another effect of these individual pumps is that individual loads have more control over the network. Furthermore, these pumps allow the network to be used for other applications than solely district heating, for instance underfloor heating and air-conditioning. Secondly, the pipe length from source to load (supply and return added together) is the same for each load. This means that each loop will have the same pressure drop and losses. This in turn makes the use of the network easier and enables a faster control system. Note that there is still one main pump to keep the pressure in the network constant.

Different time scales arise within a heating network [Kuosa et al., 2013]. The changes in pressure and flow will reach throughout the entire network within seconds and are therefore considered

instantaneous. Changes in temperature, on the other hand, travel with the flowing water and can take hours to reach the entire network. That is, temperature rises at the start of a pipe can take hours to reach the end of the pipe due to heat losses to the surroundings. Depending on the application, a dynamic or steady-state (static) approach is used. For the steady-state case, the temperature directly after the source is considered constant and the temperature over a pipe is assumed to have reached some time independent profile. For now, a steady-state approach will be considered.

2.3.2 Network representations

When representing district heating as a network, nodes and links are introduced. The nodes represent a point in the network where heat enters or leaves the network, i.e. a load or source is connected to this node. The links represents the pipes connecting these points. The representation of the network follows the representation as described by Liu [2013]. For a heating network, a node is fully described by four parameters:

- Pressure head H
- Heat power ϕ
- Supply temperature T^s
- Return temperature T^r

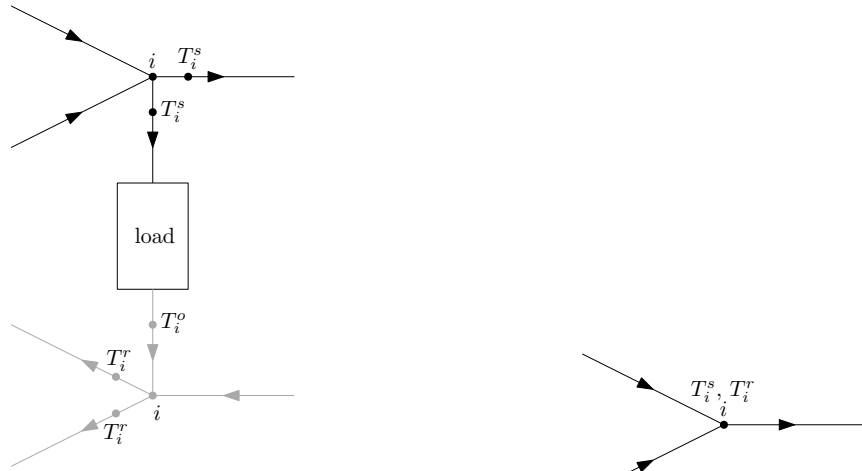
Note that there is also an outflow temperature T^o for every node with a load connected to it, but it is not needed to fully describe the node. Furthermore, there is mass flow \dot{m} , which is a link variable. It is important to note that in reality, temperature is not actually a node variable. Rather, there is a temperature distribution within a pipe (i.e. link), and the temperature of a node is taken the same as the temperature at the beginning or the end of pipe. This value is then defined as the node temperature, see also Figure 8a. For instance, the supply temperature of node i is the average of the temperatures (weighted with respect to mass flow) at the end of the two incoming pipes.

In reality, the district heating network consists of a supply and return line. For the network representation, however, it is assumed that the mass flow rate in the return line is equal in size (but opposite in direction) to the mass flow in the supply line. Therefore, each pair of supply and return line to or from a load is modeled as one link, see Figure 8a. Usually, a link in the network represents the supply line. The return line is then implicitly used to compute the return temperatures. Note that this approach only holds for the traditional Y-network. For a ring network, the supply and return lines both have to be modeled explicitly.

When seeing the temperatures as node variables and when representing both supply and return line with one link, (one node in) the network can be represented as in Figure 8b.

Three types of node can be distinguished as shown in Table 4. Note that the mass flow \dot{m} is also an unknown, but since this is an edge variable, it is not included in the table. In more detail, the following can be said about the node types:

- slack node: to ensure that the model will be well defined the pressure head must be specified at one node (see also the gas network). This node is called the slack node. Usually, a source node is taken as the slack node.



(a) Full network representation of a load (the supply line is shown in black, the return line is shown in gray). (b) Reduced network representation of a load.

Figure 8: Network representation of district heating (for a traditional network).

Table 4: Node types for the heat network

Node type	Number of nodes	Specified parameters	Unknown parameters
slack node	1	H_i	T_i^r, T_i^s, ϕ_i
source node	N_s	T_i^s, ϕ_i	T_i^r, H_i
load node	$N - N_s - 1 := N_L$	T_i^r before mixing, ϕ_i	T_i^s, H_i

- load node: at the load node it is actually T_i^o that is known, i.e. the outflow temperature directly after the load. However, using a mixing rule (see Section 2.3.3) the return temperature can be determined. In practice this means that for a load node both T^s and T^r are considered unknown.

A node that has both a load and a source connected to it is modeled as a load node.

2.3.3 Model

As mentioned before, the steady-state approach will be considered, furthermore it will be assumed that the network can be reduced such that only one link is used to represent both supply and return line (i.e. a Y-type network is assumed). The model for the heating network is split into two models; the hydraulic model and the thermal model. The hydraulic model is used to determine the nodal heads and the mass flows in the pipes. When this is known, the thermal model can be used to determine the supply and return temperatures. The two models can, however, be integrated into a single hydraulic-thermal model. The derivation of these models will mainly follow the derivation and description as in Liu [2013]. Also note that the hydraulic model is equivalent to the model used in the gas network.

Hydraulic model There are two main ways to formulate the hydraulic model; the nodal formulation or the loop formulation. The loop formulation is the most commonly used formulation and is also used in Liu [2013]. Despite the higher number of equations compared with the nodal formulation, Arsene et al. [2004] state that the loop formulation is preferred because the nodal formulation can show bad convergence behavior in situations with low pipe flow and because the loop formulation is more suitable for including pressure-controlling elements. Here, the loop formulation will be used.

The first step is the continuity of flow, which states that the sum of the mass flow entering and leaving a node must be equal to zero:

$$A\dot{m} = \dot{m}_q \quad (41)$$

where A is the $N \times N_e$ branch-nodal incidence matrix with N the number of nodes and N_e the number of edges, \dot{m} is the $N_e \times 1$ vector of mass flow within each pipe and \dot{m}_q is the $N \times 1$ vector of mass flow injected by a source (or discharged to a load). The incidence matrix is defined as follows:

$$A = \begin{cases} 1, & \text{if the flow of a pipe enters the node} \\ -1, & \text{if the flow of a pipe leaves the node} \\ 0, & \text{otherwise} \end{cases} \quad (42)$$

For \dot{m}_q it then holds that an entry is negative if there is mass injected into the node (source) and an entry is positive if mass leaves the node (load). Furthermore, \dot{m} represents mass flow, which means that if \dot{m}_{ij} is used to denote the mass flow from node i to node j , then it holds that $\dot{m}_{ij} = -\dot{m}_{ji}$. Note that the continuity of flow (41) is generally an underdetermined system, i.e. there are more unknown mass flows than there are equations. To solve this, the second part of the hydraulic model is used, assuming a loop formulation.

The second part of the hydraulic model is given by the loop pressure equation. This equation states that the sum of head losses around a closed loop must be equal to zero. This leads to following equation:

$$B\Delta H = 0 \quad (43)$$

where B is the $N_{\text{loop}} \times N_e$ branch-loop incidence matrix, with N_{loop} the number of loops, defined by:

$$B = \begin{cases} 1, & \text{if the flow in a pipe is in the same direction as the direction of the loop} \\ -1, & \text{if the flow in a pipe is in the opposite direction to the direction of the loop} \\ 0, & \text{otherwise} \end{cases} \quad (44)$$

To conclude the hydraulic model, a relation between the head loss and the mass flow is needed, which is given by the head loss equation for a pipe:

$$\Delta H = K\dot{m}|\dot{m}| \quad (45)$$

where K is the vector consisting of the resistance coefficient of each pipe. Using the head loss equation, the loop pressure equation can be rewritten to:

$$BK\dot{m}|\dot{m}| = 0 \quad (46)$$

The loop pressure equation combined with the continuity of flow gives a non-linear system of equations:

$$F(x) = \begin{pmatrix} A\dot{m} - \dot{m}_q \\ BK\dot{m}|\dot{m}| \end{pmatrix} = 0 \quad (47)$$

where F has length N_e . And the vector x of length N_e is given by:

$$x = \begin{pmatrix} \dot{m}_1 \\ \dot{m}_2 \\ \vdots \\ \dot{m}_{N_e} \end{pmatrix} \quad (48)$$

Newton-Raphson can be used to solve this system for the mass flows in each pipe.

Thermal model After the hydraulic model is used to determine the mass flows in each pipe, the thermal model can be used to determine the temperatures T^o , T^s and T^r in each node. Note that outlet temperature depends on the outdoor (i.e. ambient) temperature T^a . Both T^a and T^o are assumed to be known at each load. For simplicity, the following notation is introduced:

$$T' = T - T^a \quad (49)$$

Furthermore, it is assumed that T^s is known at each source node. Essentially, the temperature in each node is computed by ‘following the flow’, in which the temperature at the end of a pipe is computed in terms of the temperature at the start of the pipe according to a temperature profile:

$$T'_{\text{end}} = e^{\frac{-\lambda L}{C_p \dot{m}}} T'_{\text{start}} := \psi T'_{\text{start}} \quad (50)$$

where λ is the heat transfer coefficient of each pipe in $\text{W m}^{-1} \text{K}^{-1}$, L is the length of the pipe in m and C_p is the specific heat of the water in $\text{J kg}^{-1} \text{K}^{-1}$. So, if you start at the source, for which T^s is known, the supply temperatures of the other nodes can be determined by following the flow. Then the same can be done for the return line, where you start at the load at the end of the network, for which it simply holds that $T^r = T^o$. However, when a node has more than one incoming pipe, the temperature is determined by taking the weighted average of the temperatures at the end of all the incoming pipes. This is called the mixing rule:

$$\left(\sum \dot{m}_{\text{out}} \right) T_{\text{out}} = \left(\sum \dot{m}_{\text{in}} T_{\text{in}} \right) \quad (51)$$

Here, T_{out} is equal to the temperature at the node, see also Figure 8a. T_{in} is the temperature at the end of the incoming pipe, \dot{m}_{in} is the mass flow of the incoming pipe and \dot{m}_{out} is the mass flow of the outgoing pipe. This leads to the procedure as described below to determine the temperatures at each node, starting with the supply temperature.

First the mixing nodes are determined based on the network incidence matrix A . The nodes that are mixing nodes are the nodes for which the corresponding row in A has more than one entry equal to 1. For the non-mixing nodes, the pipe temperature drop equation (50) can be used, and for the mixing nodes, the mixing rule (51) is used. This leads to a linear system of equations:

$$C_s T^{sl} = b_s \quad (52)$$

where C_s is a $N - 1 \times N - 1$ matrix of coefficients, $T^{s'}$ is a vector of length $N - 1$ of supply temperatures and b_s is a vector of length $N - 1$ of solutions. Details on how to find the exact entries of C_s and b_s can be found in Liu [2013].

When all the supply temperatures are known, the return temperatures can be determined in a similar way. The incidence matrix used for the return line to determine the mixing nodes is the negative of the network incidence matrix used for the supply temperatures:

$$A^r = -A^s := -A \quad (53)$$

Every node for which the corresponding row in A^r has more than one entry equal to 1 are mixing nodes. However, there can now be some nodes for which the corresponding row has only one entry equal to 1, but which is still a mixing node. Every load node has one incoming pipe from the load, see Figure 8a, which means that if a load node has only one incoming pipe of the return line, i.e. has only one entry equal to 1 in the corresponding row of A^r , it is still a mixing node. For the load the furthest away from the source, i.e. a load for which all the pipes of the return line leave that node, it holds that $T^{r'} = T^{o'}$. For the non-mixing nodes, the pipe temperature drop equation (50) can be used, and for the mixing nodes, the mixing rule (51) is used. This leads to a linear system of equations to determine the return temperature of all loads:

$$C_r T^{r'} = b_r \quad (54)$$

where C_r is a matrix of coefficients, $T^{r'}$ is a vector of length $N - 1$ of return temperatures of all loads and b_r is a vector of length $N - 1$ of solutions. After the return temperature of all loads has been determined, the return temperature of each source can be determined using the temperature drop equation and the mixing rule. This can be done last, since in general in the return line water flows towards the sources.

Hydraulic-thermal model Instead of first using the hydraulic model to solve for the mass flows in each pipe and then using the thermal model to solve for the supply and return temperatures at each node, it is possible to solve for both the mass flows and the temperatures at the same time by combining the two models into one hydraulic-thermal model. It is assumed that the supply temperature is specified at the source and that the outlet temperature is specified at each load. Furthermore, it is assumed that the mass flow rates \dot{m}_q or the heat power ϕ is known at each node except the slack node. See also Table 4 for an overview. If the mass flow \dot{m}_q is specified at each node, the hydraulic and thermal models can be used separately. If on the other hand the heat power ϕ is specified at at least one node the combined hydraulic-thermal model is used. As for the hydraulic model, the first step in the hydraulic-thermal model is the continuity of flow (41). Then the heat power equation is introduced:

$$\phi = C_p \dot{m}_q (T^s - T^o) \quad (55)$$

where ϕ is the vector of heat powers consumed or supplied at each node. Substituting the continuity of flow in the heat power equation gives the nodal heat power:

$$\phi = C_p A \dot{m} (T^s - T^o) \quad (56)$$

This equation relates the heat power ϕ to the mass flows \dot{m} in the pipes. Using the loop pressure equations and the thermal model, Newton-Raphson can be used with the following mismatch

function:

$$\Delta F(x) = \begin{pmatrix} \Delta\phi \\ \Delta H \\ \Delta T^{s'} \\ \Delta T^{r'} \end{pmatrix} = \begin{pmatrix} C_p A \dot{m} (T^s - T^o) - \phi^{spec} \\ BK \dot{m} |\dot{m}| \\ C_s T_{load}^{s'} - b_s \\ C_r T_{load}^{r'} - b_r \end{pmatrix} = \begin{pmatrix} \text{heat power mismatch} \\ \text{loop pressure mismatch} \\ \text{supply temperature mismatch} \\ \text{return temperature mismatch} \end{pmatrix} \quad (57)$$

where ϕ^{spec} is the vector of specified values of consumed or supplied heat power for each node. Note that, as in the hydraulic model, the row of A that relates to the slack node is redundant and is removed from A . This also means that the rows in C^r and C^s relating to the slack node are removed, since these matrices are based on A . Therefore, T^s and T^r at the slack node are not directly determined via this formulation, but they can be calculated after the Newton-Raphson method is used. The unknowns for Newton-Raphson are:

$$x = \begin{pmatrix} \dot{m} \\ T_{load}^s \\ T_{load}^r \end{pmatrix} \quad (58)$$

The Jacobian is then given by:

$$J = \begin{pmatrix} \frac{\partial[\Delta\phi;\Delta H]}{\partial\dot{m}} & \frac{\partial[\Delta\phi;\Delta H]}{\partial T^{s'}} & \frac{\partial[\Delta\phi;\Delta H]}{\partial T^{r'}} \\ \frac{\partial\Delta T^{s'}}{\partial\dot{m}} & \frac{\partial\Delta T^{s'}}{\partial T^{s'}} & \frac{\partial\Delta T^{s'}}{\partial T^{r'}} \\ \frac{\partial\Delta T^{r'}}{\partial\dot{m}} & \frac{\partial\Delta T^{r'}}{\partial T^{s'}} & \frac{\partial\Delta T^{r'}}{\partial T^{r'}} \end{pmatrix} \quad (59)$$

Due the expressions used for the mismatch function the following holds for the Jacobian:

$$J = \begin{pmatrix} \frac{\partial[\Delta\phi;\Delta H]}{\partial\dot{m}} & \frac{\partial[\Delta\phi;\Delta H]}{\partial T^{s'}} & 0 \\ \frac{\partial\Delta T^{s'}}{\partial\dot{m}} & \frac{\partial\Delta T^{s'}}{\partial T^{s'}} & 0 \\ \frac{\partial\Delta T^{r'}}{\partial\dot{m}} & 0 & \frac{\partial\Delta T^{r'}}{\partial T^{r'}} \end{pmatrix} := \begin{pmatrix} J_{11} & J_{12} & 0 \\ J_{21} & J_{22} & 0 \\ J_{31} & 0 & J_{33} \end{pmatrix} \quad (60)$$

Even though $J_{21} = \frac{\partial\Delta T^{s'}}{\partial\dot{m}} \neq 0$ and $J_{31} = \frac{\partial\Delta T^{r'}}{\partial\dot{m}} \neq 0$ these two terms are generally small and can be assumed to be zero [Liu, 2013]. J_{11} is a $N - 1 \times N_p$ matrix given by:

$$J_{11} = \begin{pmatrix} C_p A (T^s - T^o) \\ 2BK |\dot{m}| \end{pmatrix} \quad (61)$$

Table 5: Equivalence between networks

General network	Kirchhoff's first law	Kirchhoff's second law	Resistance law	Transported quantity law
Gas network	Kirchhoff's first law	Kirchhoff's second law	Steady-state flow equation	-
Electrical network	Kirchhoff's current law	Kirchhoff's voltage law	Ohm's law	Complex power equation
Heating network	Continuity of flow	Loop pressure equations	Head loss equation	Heat power equation

Table 6: Equivalence between network equations

network type	Kirchhoff's first law	Kirchhoff's second law	Resistance law	Extra
Gas network	$L = A'_{\text{gas}} f$	$B_{\text{gas}} \Delta \pi = 0$	$f = \phi^{-1}(\Delta \pi)$	-
Electrical network	$I^{\text{spec}} = A'_{\text{elec}} I_{ij}$	$B_{\text{elec}} \Delta V = -A_{\text{elec}}^T V = 0$	$I_{ij} = Y \Delta V$	$S_i = V_i I_i^*$
Heating network	$\dot{m}_q = A'_{\text{heat}} \dot{m}$	$B_{\text{heat}} \Delta H = -A_{\text{heat}}^T H = 0$	$\Delta H = K \dot{m} \dot{m} $	$\phi = C_p A_{\text{heat}} \dot{m} (T^s - T^o)$

Power grid To derive a model for the power grid in analogy to the derivation of the gas network, Ohm's law is rewritten:

$$I_{ij} = Y \Delta V = Y(-A^T V) \quad (65)$$

substituting this in Kirchhoff's first law gives:

$$I^{\text{inj}} = A'_{\text{elec}} Y(-A^T V) = -A'_{\text{elec}} Y A^T V \quad (66)$$

This gives a system of equations to solve for the nodal voltages, which is the equivalence of the system for the gas network that is used to solve for the nodal pressures. In order to compute the complex power (i.e. to compute the active and reactive power), the system is substituted in the

expression for the complex power:

$$S_i = V_i I_i^* \quad (67)$$

$$= V_i (-A'_{elec} Y A^T V)_i^* \quad (68)$$

$$:= V_i (\mathcal{Y}V)_i^* \quad (69)$$

$$= V_i \sum_{k=1}^N V_k^* \mathcal{Y}_{ik}^* \quad (70)$$

$$= \sum_{k=1}^N |V_i| |V_k| (\cos \delta_{ik} + j \sin \delta_{ik}) (G_{ik} - j B_{ik}) \quad (71)$$

Heating network To derive a model for district heating in analogy to the derivation of the gas network, the head loss equation $\Delta H = K \dot{m} |\dot{m}|$ is used. This equation gives the relation between the nodal heads H and the mass flow \dot{m} in each edge and can be rewritten as:

$$\begin{aligned} \Delta H &= K \dot{m} |\dot{m}| \\ &= \text{sign}(\dot{m}) K \dot{m}^2 \\ \dot{m} &= \pm \sqrt{\frac{1}{\text{sign}(\dot{m}) K} \Delta H} \end{aligned}$$

Note that $\text{sign}(\dot{m})$ is determined by the sign of the head loss, i.e.

$$\text{sign}(\dot{m}) = \text{sign}(\Delta H) = \begin{cases} 1, & \text{if } H_i > H_j \\ -1, & \text{if } H_i < H_j \end{cases} \quad (72)$$

Since head H can be expressed in term of pressure p using $p = \rho g h$, with ρ the density, g the gravitational constant and h the height, this shows that the head loss equation is indeed equivalent to the steady-state flow equation of the gas network. To keep it general, the head loss equation will be rewritten as:

$$\dot{m} = \varphi^{-1}(\Delta H) \quad (73)$$

Substituting this in the continuity of flow, i.e. Kirchhoff's first law, gives:

$$\begin{aligned} \dot{m}_q &= A \dot{m} \\ &= A \varphi^{-1}(\Delta H) \\ &= A \varphi^{-1}(-A^T H) \\ &= A \varphi^{-1}\left(-A^T \frac{1}{\rho g} p\right) \end{aligned}$$

Which is a non-linear system of equations that can be solved for the nodal heads H (or the nodal pressures p). Note that this system only gives the hydraulic model. However, using the heat power

equation $\phi = C_p A_{\text{heat}} \dot{m} (T^s - T^o)$, this system can be extended to the hydraulic-thermal model:

$$\begin{aligned}\phi^{inj} &= C_p A_{\text{heat}} \dot{m}_q (T^s - T^o) \\ &= C_p A_{\text{heat}} A \varphi^{-1} (-A^T H) (T^s - T^o) \\ &= \left(C_p A_{\text{heat}} A \varphi^{-1} \left(-A^T \frac{1}{\rho g} p \right) \right) (T^s - T^o)\end{aligned}$$

For the Newton-Raphson method, the following can be used:

$$x = \begin{pmatrix} H_{\text{loads}} \\ T_{\text{loads}}^{s'} \\ T_{\text{loads}}^{r'} \end{pmatrix} \quad (74)$$

$$\Delta F(x) = \begin{pmatrix} \Delta \phi \\ \Delta T^{s'} \\ \Delta T^{r'} \end{pmatrix} = \begin{pmatrix} C_p A_{\text{heat}} A \varphi^{-1} (-A^T H) (T^s - T^o) - \phi^{\text{spec}} \\ C_s T_{\text{loads}}^{s'} - b_s \\ C_r T_{\text{loads}}^{r'} - b_r \end{pmatrix} \quad (75)$$

This formulation introduces some relatively complicated terms in the Jacobian matrix compared to those in the Jacobian of the commonly used hydraulic-thermal model (60). This is because in this formulation H is one of the variables, while at the same time $\Delta T^{s'}$ and $\Delta T^{r'}$ are expressions containing \dot{m} . This means that $\frac{\partial \dot{m}}{\partial H}$, i.e. $\frac{\partial \varphi^{-1}(H)}{\partial H}$, has to be computed, which will in general be more complicated than for the Jacobian (60) for which \dot{m} is used as a variable.

4 Integrated energy networks

This section describes how the different energy networks can be coupled to form one integrated energy system. First, the different commonly used components that can be used to couple the individual networks are discussed. Secondly, two ways of modeling the integrated systems are discussed; the method as described by Shabanpour-Haghighi and Seifi [2016], Abeysekera [2016] and Liu and Mancarella [2016] and the energy hub concept as introduced by Geidl and Andersson [2007].

4.1 Coupling components

In this section some components to couple the individual networks are described and the commonly used ways to model them are given. Note that there are components that couple two of the individual networks, e.g. a turbo compressor, but there are also components that couple all three of the individual networks, e.g. a combined heat and power plant (CHP). A CHP is also called cogeneration plant, since it generates two energy types namely heat and power. Therefore, CHP is a name that can be used for multiple coupling components. An overview of some of the most common coupling components is given in Table 7. Since CHP is a name used for all components that produce heat and power, it is not included in the table.

It is important to note that a logical extension of the three networks to four networks would be to include a cooling network, see e.g. Mancarella [2014] or Abeysekera [2016], which is similar to a heating network but operates at lower temperatures. An extension of a cogeneration plant or CHP would then be a trigeneration plant or CCHP (Combined Cooling, Heat and Power plant), which produces electricity, heat and cold, see e.g. Mancarella [2014]. An even further extension would be

Table 7: Coupling components between different networks. The - indicates which network delivers energy to the component, the + indicates which networks receives energy from the component, and the c indicates that the component is used for control purposes in that network.

Component	Gas	Electricity	Heat	Reference
Turbo compressor	c	-		Koch et al. [2015], Shabanpour-Haghighi and Seifi [2016], Martinez-Mares and Fuerte-Esquivel [2012]
Heat pumps		-	+	Mancarella [2014], Liu [2013] Shabanpour-Haghighi and Seifi [2016]
Gas boiler	-		+	Mancarella [2014], Shabanpour-Haghighi and Seifi [2016]
Electric boiler		-	+	Mancarella [2014], Liu [2013]
Circulation pump		-	c	Liu [2013], Pan et al. [2016]
Gas turbine	-	+	+	Liu [2013], Pan et al. [2016], Martinez-Mares and Fuerte-Esquivel [2012]
Steam turbine	(-)	+	+	Liu [2013], Pan et al. [2016]
Gas-fired generator	-	+		Shabanpour-Haghighi and Seifi [2016], Martinez-Mares and Fuerte-Esquivel [2012], An et al. [2003]
Power-to-gas	+	-		Abeysekera [2016], Clegg and Mancarella [2015]

polygeneration plants which would for instance also produce hydrogen or chemicals [Mancarella, 2014].

4.1.1 Models

In this section a description of the different components is given and some models for the coupling components will be given. Note that this list of models is far from complete, and only gives the models that are stated in the references listed in Table 7. Since the model for the turbo compressor is already given in Section 2.1.4, it will not be described again in this section.

Heat pump. A heat pump is used to transfer heat from a cooler area to a warmer one, and works in a similar way as a refrigerator. Usually a liquid refrigerant is pumped through pipes which are either underground (for a ground source heat pump) or cover a fan (for an air source heat pump). The liquid then absorbs heat from the ground or the air which it later gives of to the area that needs to be heated. Most heat pumps are reversible, meaning that they can also be used to cool an area by absorbing heat from this area and transferring it to the ground or air. In general, heat pumps are more energy efficient than boilers but they come at higher investment costs. The efficiency of a heat pump is modeled by:

$$\text{COP} = \frac{\phi_{\text{HP}}}{P_{\text{HP}}} \quad (76)$$

where COP is the coefficient of performance, ϕ_{HP} is the heat power produced in MW and P_{HP} is the electrical power consumed in MW.

Boilers. A boiler is a closed system where a liquid (usually water) is heated to a predetermined temperature. This hot water can be circulated to heat the area. There are two main types of boiler; a gas boiler and an electrical boiler. Including a partload effect, the gas boiler is modeled by [Shabanpour-Haghighi and Seifi, 2016]:

$$q_B = \frac{1}{\text{GHV}} \left(\frac{\phi_B + a_B \phi_{B,\text{max}}}{b_B} \right) \quad (77)$$

where q_B is the amount of gas consumed in $\text{m}^3 \text{h}^{-1}$, ϕ_B is the heat power produced in MW, a_B and b_B are coefficients that relate to the part load effect and GHV is the gross heating value in Wh m^{-3} .

If the partload effect is not taken into account, a gas boiler can be modeled by its efficiency:

$$q_B = \frac{1}{\text{GHV}} \left(\frac{\phi_B}{\eta_{B,\text{gas}}} \right) \quad (78)$$

where $\eta_{B,\text{gas}}$ is the boiler efficiency.

An electric boiler can be modeled by its efficiency as well:

$$P_B = \frac{\phi_B}{\eta_{B,\text{elec}}} \quad (79)$$

where P_B is the electrical power consumed in MW, ϕ_B is the heat power produced in MW and $\eta_{B,\text{elec}}$ is the boiler efficiency.

Circulation pump. A circulation pump consumes electricity to maintain a certain pressure difference between the supply and return line and is usually located at the heat source. The pump ensures that the pressure at the node farthest away is still high enough, such that there is enough pressure between the supply and return line at this node for the water to flow from supply to return line (after having given of heat at the demand located at this node). The electrical power consumed by the circulation pump P_{CP} is given by:

$$P_{\text{CP}} = \frac{\dot{m}_{\text{CP}} g H_{\text{CP}}}{10^6 \eta_{\text{CP}}} \quad (80)$$

where \dot{m}_{CP} is the mass flow through the circulation pump in kg s^{-1} , H_{CP} is the pump head in m, η_{CP} is the efficiency of the heat pump and g is the gravitational constant. Note that the electrical power P_{CP} is measured in MW.

Turbines. First note that both gas turbines and steam turbines are examples of CHP units. For the gas turbines the following relation can be used for the electrical power produced:

$$P_{\text{GT}} = \frac{\phi_{\text{GT}}}{c_m} \quad (81)$$

where P_{GT} is the electrical power produced by the gas turbine in MW, ϕ_{GT} is the (useful) heat power produced by the gas turbine in MW and c_m is the constant power to heat ratio. The amount of produced power is varied by changing the amount of consumed fuel. For a gas turbine, the power is produced by a gas-fired generator. This generator will determine the amount of gas needed. Steam turbines can be divided into two categories; condensing units and back-pressure units. For a condensing unit the produced heat is not used for the district heating, but for a back-pressure unit the produced heat can be used for a district heating network. This is done by an extraction unit, which extracts some steam from the turbine at a pressure that is allowable to the district network. An extraction unit can vary between a full condensing mode and a full extraction mode, thus enabling the variation of the ratio between produced useful electrical power and useful heat power. A back-pressure steam-turbine can be modeled as:

$$Z = \frac{\phi_{ST} - 0}{P_{con} - P_{ST}} \quad (82)$$

where Z is the ratio describing the trade-off between heat power produced and electrical power produced, which is generally between 3.9 and 8.1, ϕ_{ST} is the (useful) heat power produced in MW, P_{ST} is the electrical power produced in MW, and P_{con} is the electrical power that is generated by an extraction unit in full condensing mode, which is given by:

$$P_{con} = \eta_e F_{in} \quad (83)$$

where η_e is the electrical efficiency of the extraction unit and F_{in} is the fuel input rate in MW. Note that the fuel could be gas from the gas network.

Gas-fired generator. A gas-fired generator produces energy by burning gas. The amount of electric power produced by a generator P_{GG} is determined by the heat-rate curve:

$$HR_{GG} = a_{GG} + b_{GG}P_{GG} + c_{GG}(P_{GG})^2 \quad (84)$$

where a_{GG} , b_{GG} and c_{GG} are heat rate coefficients of the generator. The amount of fuel, in this case gas, consumed by the generator is then determined by the gross heating value:

$$q_{GG} = \frac{HR_{GG}}{GHV} \quad (85)$$

Note that different version of the heat rate curve are used. For instance, Shabanpour-Haghighi and Seifi [2016] include the valve-point effect, which means they obtain the following relation between electric power produced and amount of gas consumed:

$$q_{GG} = \frac{1}{GHV} \left(a_{GG} + b_{GG}P_{GG} + c_{GG}(P_{GG})^2 + |d_{GG} \sin(e_{GG}[P_{GG,\min} - P_{GG}])| \right) \quad (86)$$

Power-to-gas. The power-to-gas coupling components are mentioned by Abeysekera [2016], and explained by Clegg and Mancarella [2015]. Power-to-gas (P2G) uses electrolysis to convert electrical power to hydrogen, which can then be directly injected into the (natural) gas network or can first be converted to synthetic natural gas (methane) after which it can be injected into the gas network. The Dutch gas network mainly transports Groningen gas (G-gas) which consists of 82% methane, 14% nitrogen and some other higher hydrocarbons, oxygen and carbon dioxide [Wobbes, 2015]. Note

that from a system perspective the production of hydrogen and synthetic natural gas are equivalent. However, production of synthetic gas is a secondary process, meaning that the efficiency will always be lower than for the production of hydrogen only. There are technical and legislative limits on the amounts of hydrogen that can be injected into the natural gas network. Note that hydrogen has approximately 1/3 of the higher heating value (HHV) of natural gas, meaning that the total HHV of the gas in the gas network is changed when hydrogen is added to the network. This means that when the energy demand of a load stays constant the gas volume flow rate may not. The amount of gas produced by the power-to-gas unit can be modeled using an efficiency:

$$E_{P2G} = \eta_{P2G} P_{P2G} \quad (87)$$

where E_{P2G} is the energy injected into the gas network, η_{P2G} is the efficiency of the power-to-gas unit and P_{P2G} is the amount of electrical power consumed by the power-to-gas unit. To determine the (volume) flow rate of gas injected into the network, the GHV value of the injected gas can be used.

Power-to-gas units can for instance be used as a way to store excess power generated by wind turbines.

CHP Even though some of the units described above are CHP units, a model for a general CHP unit can also be used, for instance the one given in Shabanpour-Haghighi and Seifi [2016]:

$$q_{\text{CHP}} = \frac{1}{\text{GHV}} \frac{P_{\text{CHP}} + \phi_{\text{CHP}}}{\eta_{\text{CHP}}} \quad (88)$$

where q_{CHP} is the gas flow consumed by the CHP in $\text{m}^3 \text{h}^{-1}$, P_{CHP} is the active power produced by the CHP in MW, ϕ_{CHP} is the heat power produced by the CHP in MW and η_{CHP} is the total efficiency of the CHP unit. Note that GHV is the gross heating value in W h m^{-3} .

4.2 Coupling between networks

The coupling components described in the previous section allow for the different networks to be coupled into one integrated energy network system. There are multiple ways of modeling such an integrated energy system. However, to the best of the authors' knowledge, no detailed analysis of these different ways of modeling exist in literature. Moreover, there is no analysis done on how the separate networks can be coupled and what the effect of coupling would be on the system of network equations. That is, there is no analysis done on which coupling component can be connected to which types of node of the individual networks and what the effect of that coupling on the node type will be.

In the literature there are currently two ways of modeling an integrated energy system. One of the options is to explicitly collect the models of the separate networks and the coupling components into one (non-linear) system of equations. This will be called direct coupling and is done for all three networks in Liu and Mancarella [2016], Shabanpour-Haghighi and Seifi [2016] and Abeysekera [2016]. This way of integrating separate energy systems is also done by An et al. [2003] for electricity and gas and by Liu [2013] and Pan et al. [2016] for electricity and heat. Another option is to use so-called energy hubs, which are introduced by Geidl and Andersson [2007]. These energy hubs model the coupling components as input-output systems. It is important to note that both the direct coupling and the energy hub concept assume the system to be steady-state. However, this

ignores the dynamic behavior of some the coupling components and the different time scales present in the different energy networks [Abeysekera, 2016]. For instance, energy travels slower in the gas and heat networks than in a power grid. Also, both the gas and heat network have larger storage capacity than the power grid. Despite this, a steady-state system will be looked at.

In this section, both ways of modeling the integrated system are described and a comparison between the two methods is made, as a first step for an analysis regarding modeling of integrated energy systems. Note that this comparison is done with respect to modeling and with respect to solver techniques.

4.2.1 Direct coupling

Direct coupling explicitly collects all the models of the separate networks and coupling components into one (non-linear) system of equations. As mentioned before, Liu and Mancarella [2016], Shabanpour-Haghighi and Seifi [2016] and Abeysekera [2016] use direct coupling to model the integrated energy network system. All three use the models for the separate networks as described in sections 2.1.3, 2.2.3, and 2.3.3. For the heating network Liu and Mancarella [2016] and Shabanpour-Haghighi and Seifi [2016] use the hydraulic-thermal model while Abeysekera [2016] uses the hydraulic model for the integrated system, and uses the thermal model later to determine the return and supply temperatures. Abeysekera [2016] and Shabanpour-Haghighi and Seifi [2016] use the nodal formulation for the gas network. Liu and Mancarella [2016] include the loop pressure in the gas network, i.e. they use the hydraulic model as described for the district heating in Section 2.3.3 for the gas network as well. All three use the power mismatch function with polar coordinates for the electrical network. Furthermore, all three solve the resulting non-linear system using Newton-Raphson. When assuming the separate models as used by Shabanpour-Haghighi and Seifi [2016], the following mismatch function is obtained by collecting the separate models into one system of equations:

$$\Delta F(x) = \begin{pmatrix} \Delta f \\ \Delta P \\ \Delta Q \\ \Delta \phi \\ \Delta H \\ \Delta T^{s'} \\ \Delta T^{r'} \end{pmatrix} = \begin{pmatrix} q^{\text{spec}} - A'[\phi^{-1}(-A^T p)] \\ P^{\text{spec}} - \sum_{k=1}^N P_{ik} \\ Q^{\text{spec}} - \sum_{k=1}^N Q_{ik} \\ \phi^{\text{spec}} - C_p A \dot{m} (T^s - T^o) \\ BK \dot{m} |\dot{m}| \\ C_s T_{\text{load}}^{s'} - b_s \\ C_r T_{\text{load}}^{r'} - b_r \end{pmatrix} = \begin{pmatrix} \text{gas flow mismatch} \\ \text{active power mismatch} \\ \text{reactive power mismatch} \\ \text{heat power mismatch} \\ \text{loop pressure (heat network) mismatch} \\ \text{supply temperature mismatch} \\ \text{return temperature mismatch} \end{pmatrix} \quad (89)$$

where

$$x = \begin{pmatrix} p \\ \delta \\ |V| \\ \dot{m} \\ T_{\text{load}}^s \\ T_{\text{load}}^r \end{pmatrix} = \begin{pmatrix} \text{nodal pressure (gas network)} \\ \text{voltage angle} \\ \text{voltage amplitude} \\ \text{edge mass flow (heat network)} \\ \text{supply temperature} \\ \text{return temperature} \end{pmatrix} \quad (90)$$

It is important to note that the coupling components are treated as loads or sources with respect to the individual networks. This means that the coupling components are included in the $[\cdot]^{\text{spec}}$ terms in the mismatch function, i.e. the $[\cdot]^{\text{spec}}$ terms are the sum of the demand (for load nodes) or input (for source nodes) and any coupling components connected to the node. Abeysekera [2016]

and Liu and Mancarella [2016] model the coupling components by simply using an efficiency, i.e. $E^{\text{out}} = \eta E^{\text{in}}$ where E^{in} is the energy input of the coupling component, η is the efficiency and E^{out} is the energy output of the coupling component. Note that, since coupling components are being modeled, E^{in} and E^{out} are of different type, e.g. gas and electricity respectively. Furthermore, both Abeysekera [2016] and Liu and Mancarella [2016] assume that the efficiency η and either E^{in} or E^{out} are known for every coupling component. Abeysekera [2016] makes an exception when the coupling component is connected to the slack node of the electrical or heating network. In that case, the energy flow of the coupling component is a function of the state variables (the efficiency is still assumed to be known).

Shabanpour-Haghighi and Seifi [2016] on the other hand, use some of the more detailed models as described in Section 4.1.1. They assume that the heat power ϕ for every coupling component is known. For the integrated system they consider, this is sufficient to determine the power of the other energy types for all the components (for instance, they also model a gas-fired generator, which is connected to the slack nodes of the electrical and gas networks. Since it is connected to a slack node, a similar approach as in Abeysekera [2016] can be used). This means that $\Delta\phi$ is independent of the variables belonging to the gas and electrical network. Therefore, under the assumption that ϕ is known for every coupling component, the Jacobian matrix of the integrated systems is given by:

$$\begin{aligned}
 J &:= \begin{pmatrix} J_g & J_{ge} & J_{gh} \\ J_{eg} & J_e & J_{eh} \\ J_{hg} & J_{he} & J_h \end{pmatrix} \tag{91} \\
 &= \begin{pmatrix} \frac{\partial \Delta f}{\partial \pi} & \frac{\partial \Delta f}{\partial \delta} & \frac{\partial \Delta f}{\partial |V|} & \frac{\partial \Delta f}{\partial \dot{m}} & \frac{\partial \Delta f}{\partial T^{s'}} & \frac{\partial \Delta f}{\partial T^{r'}} \\ \frac{\partial \Delta P}{\partial \pi} & \frac{\partial \Delta P}{\partial \delta} & \frac{\partial \Delta P}{\partial |V|} & \frac{\partial \Delta P}{\partial \dot{m}} & \frac{\partial \Delta P}{\partial T^{s'}} & \frac{\partial \Delta P}{\partial T^{r'}} \\ \frac{\partial \Delta Q}{\partial \pi} & \frac{\partial \Delta Q}{\partial \delta} & \frac{\partial \Delta Q}{\partial |V|} & \frac{\partial \Delta Q}{\partial \dot{m}} & \frac{\partial \Delta Q}{\partial T^{s'}} & \frac{\partial \Delta Q}{\partial T^{r'}} \\ 0 & 0 & 0 & \frac{\partial [\Delta \phi]}{\partial \dot{m}} & \frac{\partial [\Delta \phi]}{\partial T^{s'}} & 0 \\ 0 & 0 & 0 & \frac{\partial [\Delta H]}{\partial \dot{m}} & \frac{\partial [\Delta H]}{\partial T^{s'}} & 0 \\ 0 & 0 & 0 & \frac{\partial \Delta T^{s'}}{\partial \dot{m}} & \frac{\partial \Delta T^{s'}}{\partial T^{s'}} & 0 \\ 0 & 0 & 0 & \frac{\partial \Delta T^{r'}}{\partial \dot{m}} & 0 & \frac{\partial \Delta T^{r'}}{\partial T^{r'}} \end{pmatrix} \tag{92}
 \end{aligned}$$

where $J_{\alpha\beta}$ is used to denote the derivative of the mismatch function corresponding to energy carrier α with respect to the variables corresponding to energy carrier β . J_α is used to denote the Jacobian corresponding to the individual network of energy carrier α . Depending on which coupling components are used, some of the terms in the J_{ge} , J_{gh} , J_{eg} and J_{eh} will be zero. Note that assuming other energy flows than the heat power ϕ to be known for the coupling component can result in a Jacobian matrix where J_{hg} or J_{he} have non-zero elements.

From a network (i.e. graph) perspective, these coupling components are modeled as being in a node, and (dimensionless) links are then connected to nodes from the other networks. For instance, a CHP can be considered to be in node 3 of the electrical network. Links are then connected for instance node 5 of the district heating and node 8 of the gas network. Note that for the gas

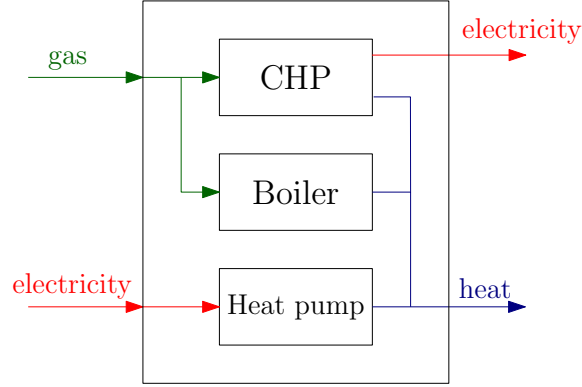


Figure 9: Example of an energy hub. It consist of a CHP, gas boiler and a heat pump.

network this link represent an outflow and for the heating network this links represents inflow. The links connecting the separate networks to the coupling components are dimensionless in the sense that they are not considered to be modeling any pipe or transmission line, i.e. no energy loss occurs over these links.

4.2.2 Energy hub

The energy hub is first introduced by Geidl and Andersson [2007] and is a way of modeling any heterogeneous network. It can therefore be used as a way of modeling any coupling component. An energy hub can be seen as an extension of a node, i.e it can be seen as a unit that has in- and outflow (like any node) but also allows for conversion and storage of different energy carriers. Therefore, an energy hub contains three main components, namely direct connections, converters and storage. Direct connection means that an energy inflow of a certain type is not converted to another energy type, i.e. the outflow is of the same type as the inflow. An example of such a direct connection would be a transmission line in the power grid or a pipeline in the gas network or heating network. Converter components convert the input energy into a different type of energy, and examples are given in Section 4.1. Storage components allow energy to be stored in order to be delivered back to the network at a later moment in time. An example of an energy hub is given in Figure 9. For the energy hub concept, the following assumptions are made [Geidl and Andersson, 2007]:

- Steady-state.
- Power flow through converters is characterized in terms of power and efficiency.
- Within an energy hub losses only occur in converter components (i.e. the links within an energy hub are assumed to be dimensionless).
- The flow through an energy hub is uni-directional.

If there is only a single converter unit, with only one type of energy input and one (other) type of energy output, the energy hub concept reduces to a simple relation using efficiency:

$$E_{\beta}^{\text{out}} = c_{\alpha\beta} E_{\alpha}^{\text{in}} \quad (93)$$

where $E_\beta^{\text{out}} \geq 0$ is the output power of energy carrier β , $E_\alpha^{\text{in}} \geq 0$ is the input power of energy carrier α and $c_{\alpha\beta}$ is the coupling factor of the conversion from energy carrier α to energy carrier β . For the very simple case considered above, the coupling factor is simply the efficiency of the converter unit. In practice, converter units do not have a constant efficiency, rather the efficiency is a function of the input power. This can be modeled by taking $c_{\alpha\beta}$ as a function of the input power E_α^{in} , i.e. $c_{\alpha\beta} = c_\beta(E_\alpha^{\text{in}})$. When combining converter components in a single energy hub, four different types can be distinguished, namely single input and single output, single input and multiple output, multiple output and single input, and multiple input and multiple output. The case for single input and single output can be described by equation (93). For the cases involving multiple input or output, this equation is extended to a matrix equation $E^{\text{out}} = CE^{\text{in}}$:

$$\begin{pmatrix} E_\alpha^{\text{out}} \\ \vdots \\ E_\omega^{\text{out}} \end{pmatrix} = \begin{pmatrix} c_{\alpha\alpha} & c_{\beta\alpha} & \cdots & c_{\omega\alpha} \\ c_{\alpha\beta} & c_{\beta\beta} & \cdots & c_{\omega\beta} \\ \vdots & \vdots & \ddots & \vdots \\ c_{\alpha\omega} & c_{\beta\omega} & \cdots & c_{\omega\omega} \end{pmatrix} \begin{pmatrix} E_\alpha^{\text{in}} \\ \vdots \\ E_\omega^{\text{in}} \end{pmatrix} \quad (94)$$

Note that the entries of the coupling matrix C are the coupling factors $c_{\alpha\beta}$. However, for an energy hub with multiple inputs or outputs, the coupling factors are not simply the converter efficiencies, rather they are a combination of the efficiencies and the dispatch factor. The dispatch factor determines how much of a certain input energy carrier is dispatched to a converter unit. If the efficiencies of the converter units in the energy hub are constant, the system of equations (94) is linear. If, however, the efficiencies depend on the input power the system of equations can become nonlinear. Furthermore, note that E^{out} and E^{in} do not necessarily have to have the same length. In general, the coupling matrix C is not invertible and the system is underdetermined. If the system (94) is indeed underdetermined, some degrees of freedom arise, meaning that optimization can be applied. If E^{out} and E^{in} have the same length, optimization is only possible if the coupling matrix C is not constant. The optimization problem is formulated as follows. The objective function is a function of the power flow between the energy hubs, which is described by the models in sections 2.1.3, 2.2.3, and 2.3.3, and a function of the input power of the energy hubs E^{in} . Note that for instance Section 2.1.3 will only give the gas flow rate between the energy hubs (i.e. on the edges). To obtain the power flow for the gas network $E_{\text{gas}} = \text{GHV}q$ can be used. The objective function can for instance be the total energy cost or the total CO_2 emission. The equality constraints of the optimization problem are given by the power flow through the energy hub (94) and by the power flow between the energy hubs, i.e. by the mismatch function $\Delta F(x) = 0$ for the individual networks. The inequality constraints are given by the lower and upper limit for the energy hub input E^{in} and by the lower and upper limit for the power flows of the individual networks. The resulting optimization problem is solved for the input power of the energy hub E^{in} and for variables x of the individual networks. This optimization problem is only solvable for certain systems, i.e. for certain cost functions and for certain models used for both the coupling matrix and for the individual networks. If the objective function is convex and all constraints are linear equations, the solution space will be convex as well and an optimal solution can be determined. If the objective function is concave or if a constraint is nonlinear (for instance the constraint describing gas flow or electrical power flow in the individual networks), the solution space is not convex. A solution can still be found, but this solution is not guaranteed to be the optimal solution. Geidl and Andersson [2007] do not derive optimality conditions for the general optimization problem as described above. They do however give optimality conditions when only one energy hub is being optimized (i.e. flow between energy hubs is not taken into account).

As mentioned above, Geidl and Andersson [2007] assume uni-directional flow, i.e. the input and output side of the energy hub are fixed. When the energy hub concept is used to model a single coupling component, this is no extra constraint since technical limitations of the coupling component determine which energy carriers are input and which are output. However, if the energy hub concept is used to model an entire region, e.g. a block of houses or a city, it could be that the energy types of the outflow and inflow of the energy hub (i.e. of the modeled region) change depending on the energy flow in the rest of the network to which the energy hub is connected. Therefore, change in direction of energy flow through an energy hub is desirable, and this is introduced by Wasilewski [2015]. Aside from incorporating change in flow direction to the energy hub concept, he also describes how energy hubs should be connected to the rest of the network from a network (i.e. graph) perspective.

From the descriptions above it can be concluded that direct coupling is used to perform steady-state power flow analysis. In order to do this, the input or output energy of the coupling components is assumed to be known when the coupling component is not connected to a slack node. However, if this input or output energy would not be assumed known, degrees of freedom are created and optimization could be used as is done for the energy hubs.

The energy hub concept, on the other hand, models heterogeneous networks as input/output systems. This means that the energy hub model could be used for both a single coupling component as well as for an entire city. The energy hub concept generally leads to an underdetermined system of equations, such that optimization is possible. However, if the input or output energy of the energy hub would be assumed known, steady-state analysis could be used as is done for direct coupling.

5 Summary

There are different formulations for the models of the separate networks. However, a certain equivalence exists between the network equations and parameters of these individual networks, e.g. all have flow and potential variables and all obey Kirchhoff's laws. Furthermore, different types of coupling components exist, which means that the individual networks can be coupled in a variety of ways, and for most of the coupling component multiple models exist. This means that modeling the integrated energy system can be complicated. Currently two ways of modeling the integrated systems exist, namely direct coupling and the energy hub concept. However, a systematic analysis of how the individual networks can be coupled, what the effect of coupling is on the node types, and how the resulting integrated network can be modeled is not yet available.

References

- M. Abeysekera. *Combined Analysis of Coupled Energy Networks*. PhD thesis, Institute of Energy, Cardiff School of Engineering, Cardiff University, 2016.
- L. Wobbes. Smart gas grids: Technology and policy aspects. *TU Delft report*, 2015.
- A.J. Osiadacz. *Simulation And Analysis Of Gas Networks*. E. & F.N. Spon Ltd, London, 1987.
- T. Koch, B. Hiller, M. Pfetsch, and L. Schewe. *Evaluating Gas Network Capacities*. MOS-SIAM, Philadelphia, 2015.
- S. An, Q. Li, and T. Gedra. Natural gas an electricity optimal power flow. *IEEE*, 2003.
- A. Martinez-Mares and C. Fuerte-Esquivel. A unified gas and power flow analysis in natural gas and electricity coupled networks. *IEEE Transaction on Power Systems*, 27, 2012.
- A. Shabanpour-Haghighi and A.R. Seifi. An integrated steady-state operation assessment of electrical, natural gas, and district heating networks. *IEEE Transactions on Power Systems*, 31: 3636–3647, 2016.
- P. Schavemaker and L. Van der Sluis. *Electrical power systems essentials*. John Wiley & Sons LTD, West Sussex, 2008.
- B. Sereeter, C. Vuik, and C. Witteveen. On a comparison of newton raphson solvers for power flow problems. *TU Delft report*, 2016.
- R. Idema. *Newton-Krylov Methods in Power Flow and Contingency Analysis*. PhD thesis, Delft University of Technology, 2012.
- R. Wolfson. *Essential University Physics*. Pearson Addison-Wesley, San Fransisco, 2007.
- X. Guoyu. Decoupled economic dispatch using the participation factors load flow. *IEEE Transactions on Power Apparatus and Systems*, 104(6):1377–1384, 1985.
- A.C. Exposito, J.L.M. Ramos, and J.R. Santos. Slack bus selection to minimize the system power imbalance in load-flow studies. *IEEE Transactions on Power Systems*, 19:987–995, 2004.
- Agentschap NL Ministerie van Economische zaken , Landbouw en Innovatie. Stadsverwarming.
- S. Frederiksen and S. Werner. *District Heating and Cooling*. Studentlitteratur AB, Lund, 2013.
- M. Kuosa, K. Kontu, T. Mäkilä, M. Lampinen, and R. Lahdelma. Static study of traditional and ring networks and the use of mass flow control in district heating applications. *Applied Thermal Energy*, 54:450–459, 2013.
- X. Liu. *Combined Analysis of Electricity and Heat Networks*. PhD thesis, Institute of Energy, Cardiff University, 2013.
- C.T.C Arsene, A. Bargiela, and D. Al-Dabass. Modelling and simulation of water systems based on loop equations. *I.J. of Simulation*, 5, 2004.

- X. Liu and P. Mancarella. Modelling, assessment and sankey diagrams of integrated electricity-heat-gas networks in multi-vector district energy systems. *Applied Energy*, 167:336–352, 2016.
- M. Geidl and G. Andersson. Optimal power flow of multiple energy carriers. *IEEE Transaction on Power Systems*, 22, 2007.
- P. Mancarella. Mes (multi-energy systems): An overview of concepts and evaluation models. *Energy*, 65:1–17, 2014.
- Z. Pan, Q. Guo, and H. Sun. Interactions of district electricity and heating systems considering time-scale characteristics based on quasi-steady multi-energy flow. *Applied Energy*, 167:230–243, 2016.
- S. Clegg and P. Mancarella. Integrated modeling and assessment of the operational impact of power-to-gas (p2g) on electrical and gas transmission networks. *IEEE Transactions on Sustainable Energy*, 6:1234–1244, 2015.
- J. Wasilewski. Integrated modeling of microgrid for steady-state analysis using modified concept of multi-carrier energy hub. *Electrical Power and Energy Systems*, 73:891–898, 2015.